

Accepted Manuscript

Design, synthesis and biological evaluation of novel pyrazolochalcones as potential modulators of PI3K/Akt/mTOR pathway and inducers of apoptosis in breast cancer cells

Anver Basha Shaik, Garikapati Koteswara Rao, G. Bharath Kumar, Nibedita Patel, Vangala Santhosh Reddy, Irfan Khan, Sunitha Rani Routhu, C. Ganesh Kumar, Immadi Veena, Kunta Chandra Shekar, Madan Barkume, Shailesh Jadhav, Aarti Juvekar, Jyoti Kode, Manika Pal-Bhadra, Ahmed Kamal

PII: S0223-5234(17)30578-0

DOI: [10.1016/j.ejmech.2017.07.056](https://doi.org/10.1016/j.ejmech.2017.07.056)

Reference: EJMECH 9619

To appear in: *European Journal of Medicinal Chemistry*

Received Date: 26 March 2017

Revised Date: 25 June 2017

Accepted Date: 23 July 2017

Please cite this article as: A.B. Shaik, G.K. Rao, G.B. Kumar, N. Patel, V.S. Reddy, I. Khan, S.R. Routhu, C.G. Kumar, I. Veena, K. Chandra Shekar, M. Barkume, S. Jadhav, A. Juvekar, J. Kode, M. Pal-Bhadra, A. Kamal, Design, synthesis and biological evaluation of novel pyrazolochalcones as potential modulators of PI3K/Akt/mTOR pathway and inducers of apoptosis in breast cancer cells, *European Journal of Medicinal Chemistry* (2017), doi: 10.1016/j.ejmech.2017.07.056.

This is a PDF file of an unedited manuscript that has been accepted for publication. As a service to our customers we are providing this early version of the manuscript. The manuscript will undergo copyediting, typesetting, and review of the resulting proof before it is published in its final form. Please note that during the production process errors may be discovered which could affect the content, and all legal disclaimers that apply to the journal pertain.



Design, Synthesis and Biological Evaluation of Novel Pyrazolochalcones as Potential Modulators of PI3K/Akt/mTOR Pathway and Inducers of Apoptosis in Breast Cancer Cells

Anver Basha Shaik,¹ Garikapati Koteswara Rao,² G. Bharath Kumar,¹ Nibeditha Patel,² Vangala Santhosh Reddy,¹ Irfan Khan,¹ Sunitha Rani Routhu,¹ C. Ganesh Kumar,¹ Immadi Veena,² Kunta Chandra Shekar,¹ Madan Barkume,³ Shailesh Jadhav,³ Aarti Juvekar,³ Jyoti Kode,^{*3} Manika Pal-Bhadra,^{*2} Ahmed Kamal^{*1}

¹Medicinal Chemistry and Pharmacology, ²Centre for Chemical Biology, CSIR - Indian Institute of Chemical, Technology, Hyderabad, 500007, ³Anti-Cancer Drug Screening Facility (ACDSF), Advanced Centre for Treatment, Research & Education in Cancer (ACTREC), Tata Memorial Centre, Kharghar, Navi Mumbai 410210, India.

Abstract: Cancer has been established as the “Emperor of all maladies”. In recent years, medicinal chemistry has focused on identifying novel anti-cancer compounds; though discovery of these compounds appears to be a herculean task. In present study, we synthesized forty pyrazolochalcone conjugates and explored their cytotoxic activity against a panel of sixty cancer cell lines. Fifteen conjugates of the series showed excellent growth inhibition (**13b-e**, **13h-j**, **14c-d**, **15 a**, **15 c-d**, **16b**, **16d** and **18f**; GI₅₀ for MCF-7: 0.4 – 20 μM). Conjugates **13b**, **13c**, **13d**, **16b** and **14d** were also evaluated for their cytotoxic activity in human breast cancer cell line (MCF-7). The promising candidates induced cell cycle arrest, mitochondrial membrane depolarization and apoptosis in MCF-7 cells at a 2 μM concentration. Furthermore, inhibition of PI3K/Akt/mTOR pathway-regulators such as PI3K, p-PI3K, p-AKT, and mTOR were observed; as well as upregulation of p-GSK3β and tumor-suppressor protein, PTEN. Our study indicates that pyrazolochalcone conjugates could serve as potential leads in the development of tailored cancer therapeutics.

Key Words: Apoptosis, cytotoxicity, PI3K/Akt/mTOR signaling pathway, molecular modeling, Pyrazolochalcones.

1. Introduction

There has been considerable development in the synthesis of antiproliferative drugs that inhibit the function of various proteins. Phosphatidylinositol-3-kinases (PI3Ks) are a family of lipid kinases characterized by their ability to phosphorylate the 3'-OH group in the ring of inositol phospholipids.^[1] PI3Ks are involved in a number of cellular processes including cell growth, proliferation, nutrient uptake, differentiation, motility, survival, and intracellular trafficking. The well characterized members of this family are class I PI3Ks (α , β , γ and δ isoforms) that link PI3K activity to a large variety of cell-surface receptors, including growth factor receptors and G protein-coupled receptors (GPCRs). Class I PI3Ks are heterodimers composed of a catalytic subunit (p110) and an adaptor/regulatory subunit (p85). There is significant evidence that the PI3K/Akt/mTOR pathway is crucial to the survival of many human cancer cells and regulates cell metabolism as well as proliferation.^[2-3] Aberrant activation of this pathway is considered important in the initiation and maintenance of human tumors. This signaling cascade includes a number of proteins and therefore provides numerous targets for inhibition.^[4]

PF-04691502 (**1**) bearing pyridopyrimidinone acts as a dual inhibitor of PI3K/mTOR kinase resulting in induced apoptosis and anti-proliferation of cancer cells.^[5] Wortmannin (**2**) and LY294002 (**3a**) (**Figure 1**) are potent nonselective inhibitors of PI3Ks which also demonstrate inhibitory effects on targets not related to PI3K family.^[6-8] Quercetin (**3b**) and tangeretin (**3c**) (**Figure 1**) flavonoids reported to exhibit anti-carcinogenic and chemopreventive activities by inducing apoptosis apart from impeding the function of critical growth factors.^[9-11] Moreover, adriamycin (**4**) (**Figure 1**) a well-known chemotherapeutic drug, inhibits cell growth by interacting with DNA to induce apoptosis.^[12]

Pyrazoles are well recognized conjugates of biological importance and are considered versatile building blocks in the fields of organic and medicinal chemistry.^[13] Recently, some scaffolds like pyrazole restricted CA-4 (**5a**) dihydropyridopyrazoles (**5b**) and flavokawain B (FKB) (**6**) have shown potential antiproliferative action, as well as apoptosis inducing properties apart from antitubulin activity.^[14-15] Notably, pyrazole derivatives received attention as chemotherapeutic agents due to their remarkable effect on cellular targets like p38 α MAP kinase (**5c**)^[16] p53-MDM2 and NF- κ B,^[17] topoisomerase I, STAT3 phosphorylation,^[18] sirtuin (SIRT1 and SIRT2)^[19] and PI3K.^[20] Additionally, pyrazole-based pyrrolidinyl pyridopyrimidinone derivatives have been reported as dual inhibitors of PI3K α and mTOR.^[21] It is noteworthy to

mention that the pyrazole containing NSC-45410 is currently considered for preclinical reassessment as a cytotoxic agent.^[22-25] Chalcones are also important bioactive molecules known to exhibit cytotoxicity by modulating cellular targets like EGFR,^[26] ODC,^[27] NF- κ B, proteasome,^[28] and Nrf2/ARE.^[29] SD400 (**7**) inhibited the growth of P388 murine leukemia cell line at a low concentration (IC₅₀, 2.6 nM).^[30-33] Despite the numerous efforts in developing novel antitumor agents that modulate apoptotic markers, many drugs currently under clinical investigation are still limited by critical restrictions. Specifically, occurrence of peripheral neuropathy and acute toxicity are major limitations in the development of PI3K/Akt/mTOR modulators and apoptosis inducers as cancer drugs.^[34-37] Therefore, novel chemotherapeutic design must still overcome the challenges posed by multi-drug resistance, neuropathies and acute toxicity.^[38-39]

Structural combinations of two pharmacophores significantly impart antiproliferative activity to the designed molecules.^[40] In light of these facts and to achieve some innovative molecules with remarkable cytotoxicity, this study illustrates the synthesis of novel pyrazolochalcone hybrids as chemotherapeutic agents that profoundly induce apoptosis. Thus, a set of conjugates with different groups like OCH₃, OCH₂O, Cl, and F as phenyl ring substituents were generated and their structure-activity relationships (SAR) evaluated. It is noteworthy to mention that this forms the first report wherein pyrazolochalcone derivatives have been systematically synthesized and were examined for their cytotoxic potency against a panel of 60 cancer cell lines (NCI developmental therapeutic program), (International Patent: WO2015029051 A1).^[41] Significantly, conjugates **13b**, **13c**, **13d**, **14d** and **16b** exhibited promising activity which prompted us to assess their prospective role in controlling cell proliferation and apoptosis in human breast cancer cells (MCF-7). We considered evaluating their mode of action on cell cycle progression as well as cell survival. Fascinatingly, cell signaling pathway demonstrated that they are potential modulators of PI3K/AKT/mTOR targets leading to induced apoptosis. To validate the mechanism, we evaluated the effect on mitochondrial membrane potential as a measure of early induction of intrinsic apoptosis. PI3K, docking simulations depicted that they occupy ATP binding site of PI3K γ . To gain more insight into these findings, the promising conjugates were studied for their acute toxicity (data not shown). These findings led to a new paradigm for the pharmacological use of pyrazolochalcones in the treatment of human breast cancer.

<Insert figure 1 here>

2. Results and discussion

2.1. Chemistry: Synthesis of pyrazolochalcones is outlined in Schemes 1, 2 and 3, wherein the final step has been carried out by the application of Claisen–Schmidt condensation between equimolar mixtures of 3-phenyl-1*H*-pyrazole-5-carbaldehydes (**12a-d**) and substituted acetophenones/indanones in the presence of base in ethanol. The key intermediates 3-substituted phenyl-1*H*-pyrazole-5-carbaldehydes (**12a-d**) were individually prepared in four sequential steps. Initially, the substituted acetophenones (**8a-d**) were oxylated in presence of sodium ethanolate in ethanol yielded ethyl 2,4-dioxo-4-(substituted phenyl)butanoates (**9a-d**). These diketo esters were further cyclised with NH₂-NH₂·2HCl in refluxing ethanol to result ethyl 3-substituted phenyl-1*H*-pyrazole-5-carboxylates (**10a-d**) and these carboxylates were reduced to corresponding pyrazole alcohols **11a-d** by LiAlH₄. These were selectively oxidized to 3-substituted phenyl-1*H*-pyrazole-5-carbaldehydes (**12a-d**) by IBX in DMSO.⁴²⁻⁴³ The final target conjugates obtained were characterized by IR, ¹H NMR, ¹³C NMR, mass and HRMS spectral data, wherein the α,β-unsaturated carbonyl protons (*trans H*) were confirmed by coupling constant (*J* = 14-18 Hz). All the synthesized compounds have >95% purity as determined by high-performance liquid chromatography (HPLC).

<Insert scheme 1-3>

3. Biological results

3.1.1. Cytotoxicity

The newly synthesized conjugates of pyrazolochalcones bearing various substituents on the A and C-rings were initially evaluated for their cytotoxicity in a panel of sixty human cancer cell lines (leukemia, non-small cell lung, colon, CNS, melanoma, ovarian, renal, prostate and breast cancer) as per NCI protocol. Our data suggest that the A-ring decorated with electron donating substituents (OCH₃)₃, (OCH₃)₂, (OCH₃), and 3,4(-OCH₂O-) whereas the C-ring contains both electron donating as well as withdrawing groups (OCH₃, 3,4(-OCH₂O-), NH₂, H, Cl, Cl₂ and F₂) (Figure 1). Among them, 27 conjugates were taken up for single dose (10 μM) screening and the conjugates **13 (b-e, h-j)**, **14(c-d)**, **15 (a, c-d)**, **16 (b, d)** and **18f** showed significant activity in the preliminary screening. When subjected to five dose screening (0.01, 0.1, 1.0, 10, 100 μM), conjugates like **13b-d**, **14c-d**, **15a**, **15c-d**, **16b** and **16d** showed broad cytotoxic activity against cancer cell lines with GI₅₀ values of 0.18-5.5 μM. Interestingly, SR and RPMI 8226 cells of leukemia type were particularly affected by these conjugates with GI₅₀ value

<1 μM . Moreover, **13b**, **13c**, **13d**, **13e** and **13j** with a trimethoxy phenyl pharmacophore as A-ring and electropositive substituents (OCH_3 , OCH_2O and NH_2) on the C-ring elicit pronounced cytotoxicity with the GI_{50} values of 0.34 μM (SR), 0.18 μM (NCI522), 0.31 μM (RPMI 8226), 0.55 μM (SR) and 0.32 μM (SR), respectively. In comparison, conjugates **13h** and **13i** functionalized with same unit on the A-ring and electronegative (Cl_2 and F_2) substitutions on the C-ring exhibited less potency (GI_{50} = 0.39 μM and 2.92 μM in SR cells). In addition, conjugates **15a**, **15c** and **15d** decorated with dimethoxy units on A-ring and similar electropositive groups on their C-ring demonstrated potential activity in SR cells with the GI_{50} values of 0.20 μM , 0.25 μM and 0.58 μM , respectively. However, 3,4-(methylenedioxy) (**14c-d**) and monomethoxy (**16b**, **16d**) substitution on the A-ring and a common electropositive group on the D-ring also established significant cytotoxicity in sub-micromolar levels; however, in lesser magnitude when compared to **13b-d**.

<Insert Table 1 here>

A total 40 compounds were also evaluated for their antiproliferative activity against human breast cancer cell lines, MCF-7 and MDA-MB-231 (**Table 2**) employing adriamycin and CA-4 as standards. Most of them exhibited potential cytotoxicity in both the breast cancer cells with IC_{50} values of <1 μM . Conjugates **13b**, **13c** and **13d** preferentially inhibited the growth of MCF-7 cells with an IC_{50} of 0.81 μM , 0.51 μM and 0.43 μM , respectively, indicating that potency had been increased with an increase in the number of methoxy units on the C-ring. Similarly, conjugates **13e**, **14c-d**, **15a-b** and **16b** possessing 3,4-(methylenedioxy), di- and trimethoxy substitutions on their C-ring also demonstrated pronounced growth inhibition. Whereas, conjugates **13h** (IC_{50} = 3.2 μM) and **13i** (IC_{50} = 2.5 μM) containing electronegative chloro and fluoro groups on the C-ring, suffered from a reduction in observed potency. Therefore, the optimal activity order of substitutions on the C-ring is $(\text{OCH}_3)_3 > (\text{OCH}_3)_2 = 3,4-(\text{OCH}_2\text{O}-) > \text{OCH}_3 > \text{NH}_2 > \text{H} > \text{F}_2 > \text{Cl}_2 > 3\text{-F}, 4\text{-OCH}_3 > \text{Cl}$ (Figure 1). Additionally, conjugates **17**, **18 (a-f)** with cyclic acetones have shown moderate to good cytotoxicity. Interestingly, **17a-f** anchorage with trimethoxy substitutions on A-ring displayed enhanced potency when compared to **18a-f** that contain 3,4-(methylenedioxy) group on the A-ring. Wherein, the presence of methoxy substitutions on the C-ring **17e-17f** (2.1 μM , and 2.0 μM), **18e-18f** (2.7 μM and 1.7 μM) showed considerable IC_{50} values in MCF-7 cells. Overall, the conjugates **13b-d**, **14c-d**, **15a**, **15c-d**, **16b**

and **16d** that demonstrated potential cytotoxicity in the NCI 60 cell line study also showed similar effects in MTT assay.

<Insert Table 2 here>

3.1.2. Effect on intrinsic apoptotic pathway

To examine the potential role of these conjugates in triggering early apoptosis, MCF-7 cells were treated with **13c**, **13d**, **16b** and **14d** for 18 h at 2 μ M and then stained with DiOC6. Intrinsic apoptosis was detected as early as 5 h (3.4% for **14d** and 7.6% for CA-4) which increased after 18 h incubation of MCF-7 cells with conjugates that were 26% for **14d** and **16b**. Moreover, **13c** exhibited extensive level of induction of intrinsic apoptosis with 42%, while the positive control CA-4 with 46% cells with depolarized mitochondria (**Figure 2A**). However, diminished effect on mitochondrial membrane potential was observed in response to treatment with **13d**. As evident in Figure 2 (panels A-C) at 18 h, the conjugates **13b**, **16b** and **14d** induced significant mitochondrial membrane depolarization in MCF-7 cells, whereas, **13d** significantly induced hyperpolarisation at 18 h. It is reported that hyperpolarisation is a step prior to destabilization and progresses eventually to depolarization later. Therefore, this data suggests that these conjugates play a crucial role in the alteration of mitochondrial membrane potential resulting in the initiation of intrinsic apoptosis (**Figure 2**).

<Insert figure 2>

3.1.3. Effect on cell cycle progression

To gain further evidence regarding the role of these conjugates in the induction of apoptosis, we measured the cellular arrest in different phases of the cell cycle. Thus, MCF-7 cells were treated with **13c**, **13d**, **16b** and **14d** at 2 μ M for 24 h and 48 h. Normal lymphocyte DNA was used to set diploid G0-G1 phase and the untreated cells exhibited significant arrest in synthetic S-phase. Flow cytometric analysis of synchronous cells showed that the majority of cells were arrested in G2-M phase of the cell cycle at 24 h ranging from 15.3% to 39.9% (**Figure 3A (e-h) and 3B**). Additionally, the conjugates **13c** and **14d** at 24 h induced a profound block in G0-G1 phase by 30.8% and 61.9%, respectively. Wherein, at 48 h, the conjugates **13b**, **13d**, **16b** and **14d** demonstrated a distinct tendency to block cell growth at G0-G1 (39% to 62%). Intriguingly, **13d** with trimethoxy groups on both phenyl rings showed a pronounced cell arrest at G0-G1 phase by 62% as compared to that of positive control ADR (59.1%) at 48 h. The

induced apoptosis was determined by measuring the percent of cells stalled in the sub-G1 peak: 31 and 44% of cells were found in the sub-G1 peak after a 48 h exposure of significant conjugates. Whereas the positive controls CA-4 and ADR at 24 h accumulate the cells at G2-M and G0-G1 stages, respectively, which continued at 48 h incubation (**Figure 3A and 3C-c,d**).

<Insert figure 3>

3.1.4. Detection of apoptosis by Annexin V-FITC and Propidium iodide staining

Therefore, extrinsic as well as intrinsic apoptosis in cells was induced by conjugates **13c**, **13d**, **16b** and **14d** were also evaluated by Annexin V-FITC and PI staining. In this study MCF-7 cells were incubated with conjugates at 2 μ M concentration for 24 h. Interestingly, all the conjugates induced early apoptosis in MCF-7 at 24 h, while the promising conjugates **13d** (11%) and **14d** (8%) preferentially showed enhanced late apoptotic induction over the control. In addition, these conjugates induced necrosis in MCF-7 cells to a maximum percent, whereas **13c** displayed a diminished effect on necrosis. Moreover, the apoptotic cells (range 5.5%-14.3%) were noticed in all the treatments of conjugates and supported our hypothesis that these conjugates inhibited the cell growth at 24 h. Cumulatively, **13d** induced apoptosis with 14.3%, whereas **14d** with 9.3% took the second place in effect and the results are compared with CA-4 (**Figure 4**). Wherein, the conjugates **13c** and **16b** exhibited a reduced effect in the induction of apoptotic cell death with 5.5% and 5.6%, respectively.

<Insert figure 4>

3.1.5. Effect on PI3K/Akt/mTOR pathway

To unravel the molecular mechanism as to how these conjugates induced apoptosis in cancer cells and to identify the implicated signaling pathway targets, Western blotting experiments were performed after isolating the total proteins from both untreated and treated MCF-7 cells with **13b**, **13c**, **13d**, **16b** and **14d** for 24 h. These blots were hybridized with antibodies for known PI3K/Akt/mTOR pathway regulators that include PI3K, Akt, p-Akt, mTOR, and GSK-3 β . A concordant decrease in the expression of PI3K, Akt (Figure 5A), p-Akt and mTOR proteins was observed in the treatments as compared to untreated cells, whereas a significant increase in the expression of p-GSK-3 β (ser-9) and PTEN were observed upon treatment (**Figure 5B**) was noticed. In a separate experiment, conjugate treated MCF-7 cells were stained with anti-Akt antibody conjugated with Alexa dye and visualized via immunofluorescence microscopy and the data corroborated with western blotting results. Akt

expression in conjugate-treated MCF-7 cells varied based on potency of the conjugates. In conclusion, both studies indicated that **13c**, **16b** and **14d** demonstrated significant downregulation of PI3K, Akt and mTOR, whereas p-GSK-3 β (ser 9) and PTEN protein levels were significantly increased. Further to investigate the mRNA levels of PI3K(110a), Akt1, PTEN of PI3K Akt axis and Bcl-2, BAX, TP53 of apoptosis related genes, we performed qRT-PCR and results indicated that the clear decrease in PI3K, Akt1 and Bcl-2 mRNA levels and significant increase of PTEN, BAX and TP53 mRNA levels upon compound treatment (**Figure 5C**).

<Insert figure 5>

3.2. Molecular modeling

In order to have a more precise picture of the interaction mode of these promising conjugates as phosphatidylinositol 3-kinase (PI3K) inhibitors, we performed molecular docking simulations for **13c**, **13d**, **14d** and **16b** with the PI3K catalytic subunit (PDB 1E7V) as a template.^[44] Docking analysis revealed that these conjugates occupied the same site corresponding to specific PI3K inhibitor LY294002 at ATP binding position of PI3K γ . Generally, the ATP binding site of PI3K is positioned in a cleft between smaller N- and the larger C-terminal lobes of the catalytic domain. Most of the PI3K inhibitors have shown potential hydrogen bonding interactions with hinge residues, Val883 and Tyr867. In the case of LY294002, the morpholine ring hydrogen-bonds to hinge residue Val882 and the edge of the morpholine ring interacts with the face of Tyr867 (Toledo et al., 1999). In the present study, all the docked conjugates encompass potential amino acid residues of both N, C-lobes, like Val882, Ala885, Lys883, Asp884, Ser806, Glu880, Tyr867, Ala805, Leu848, Lys800, Lys808, Asp964, Gly958, Asn951, Asn954, Val941, Ile1002, Met953 and showed maximum interactions with the receptor pocket. **13c** with a trimethoxy group on the A-ring and dimethoxy substituent on the C-ring showed more molecular interactions explaining pronounced inhibition of kinase function. A strong hydrogen bonding was observed between C3 methoxy O of C-ring and OH of Ser806 (O---HO, distance: 3.0 Å). In addition, C3 methoxy O of A-ring develops hydrogen bonding with NH of Asp884 (O---HN, distance: 3.0 Å) as well as NH of Lys883 (O---HN). Moreover, the dipole interactions were observed between the carbonyl O of Val882 and pyrazole N atom (N---O=C). Further, a weak hydrogen bond between carbonyl O of enone unit and NH of Asp964 (C=O---HN) was also noticed. However, the S of Met953 formed weak electrostatic interactions with NH of pyrazole

ring (S---HN). Additionally, **13c** also exhibited some hydrophobic interactions with Ile963, Ile828 and Phe783 apart from π - π stacking of Trp812 with trimethoxyphenyl A-ring. The probable interactions of **13c** with the catalytic domain harbouring significant residues (stick model) are visualized in mesh representation and the superimposition of **13c** on LY294002 also showed a reference site (Figure 6 Panel 1). Furthermore, some crystal structure poses of **13c** in catalytic domain of PI3K revealed that the docking simulations at catalytic site are identical to the known inhibitor (Figure 6 Panel 1).

<Insert figure 6>

Docking of **13d** with trimethoxy substituent on the A and C-rings develops a strong hydrogen bonding between pyrazole NH and carbonyl O of Val882 (NH---O). Additionally, the N atom of pyrazole showed a dipole interaction with O of Ala885 (N---O); however, another dipole interaction was found between carbonyl O of enone and carbonyl O of Glu880 (C=O---O=C). Moreover, both C3 and C4 methoxy O atoms formed weak hydrogen bonds with NH of Asp964. (O---NH---O) and the C5 methoxy O of same ring developed a strong hydrogen bond with phenolic H of Tyr867 (H---O). These significant hydrogen bonds at C ring of **13d** probably made the moiety to deviate from the active catalytic site demonstrating a reduced inhibitory effect. The docking pose of **14d** showed potential hydrogen bonding between pyrazole NH and carbonyl O of Val882 (NH---O), methylenedioxy O of A-ring and NH of Asp964 (O---HN) as well as dipole interactions between carbonyl O of enone and carbonyl O of Ala885 (C=O---O=C). Additionally, the hydrophobic interactions with Val941, Asn954, Ile1002 include a π - π stacking between Phe1009 and trimethoxyphenyl group of C-ring. However, **16b** formed two hydrogen bonding interactions between carbonyl O of Val882 and pyrazole NH (O---HN), and NH of same residue with O of enone carbonyl unit (NH---O). However, a weak hydrogen bond was noticed between NH of Asp964 and C4 methoxy O of C-ring. Interestingly, the dipole interaction between pyrazole N and O of Ala885 (N---O) include some hydrophobic interactions with Lys800, Glu880 and Asn951. Notably no significant interactions were noticed at A-ring of **16b** suggesting a minimum activity. Therefore, these findings reveal that pyrazolochalcones specifically occupy the ATP binding site of PI3K γ and exhibit significant molecular docking simulations with adjoining amino acids (Figure 6 Panel 2).

<Insert figure 7>

4. Conclusion

In summary, a library of pyrazolochalcones functionalized with various methoxy substituents on the phenyl ring were successfully synthesized and screened for their cytotoxicity on sixty cancer cell lines. Among them a total of fifteen compounds have shown remarkable potency towards tested cell lines with IC_{50} values $<1 \mu\text{M}$. Most active compounds (**13c**, **13d**, **16b** and **14d**) were further evaluated for their mechanistic action using assays in MCF-7 cells. These conjugates evidently exhibited G_2 -M arrest At 24 h, while after 48 h the cells were found to show G_0 - G_1 growth arrest. Furthermore, Annexin-PI staining and western bolt analysis revealed that both intrinsic as well as extrinsic apoptosis could be induced by these conjugates. Additionally, **13d** and **14d** also demonstrated increased early as well as late apoptotic cells though to a lesser extent. The promising conjugates showed distinct downregulation of PI3K, Akt and mTOR proteins along with significant upregulation of p-GSK-3 β (ser 9) and PTEN proteins. In consistency with these findings, we also observed activation of caspase-3 and caspase-9 involved in mitochondrial membrane disruption. To support this hypothesis, docking at the ATP binding site of PI3K γ exhibited significant interactions. This forms the first study where pyrazolochalcone conjugates have been synthesized and found to be efficient inducers of pro-apoptotic signalling, and inhibitors of the PI3K/Akt/mTOR pathway. Further exploration of these conjugates, possessing pyrazole and chalcone moieties, for chronic toxicity and efficacy in-vivo, may help to advance the development of tailored cancer therapeutics.

5. Experimental methods

5.1. General experimental conditions

All chemicals and reagents were obtained from Aldrich (Sigma–Aldrich, St. Louis, MO, USA), Lancaster (Alfa Aesar, Johnson Matthey Company, Ward Hill, MA, USA), or Spectrochem Pvt. Ltd. (Mumbai, India) and were used without further purification. Reactions were monitored by TLC performed on silica gel glass plates containing 60 GF-254, and visualization was achieved by UV light or iodine indicator. Column chromatography was performed with Merck 60–120 mesh silica gel. ^1H NMR spectra were recorded on Bruker UXNMR/XWIN-NMR (300 MHz) or Inova Varian-VXR-unity (400, 500 MHz) instruments. ^{13}C NMR spectra were recorded on Bruker UXNMR/XWIN-NMR (75 MHz) instrument. Chemical shifts (δ) are reported in ppm downfield from an internal TMS standard. Purity was evaluated by analytical HPLC using a LC-20AD-SHIMADZU. Mobile phase: Methanol–water (80:20, v/v) (buffer: ammonium acetate, pH 4.2) PDA detector. The column used was Phenomenex Luna (C-18) 250 x 4.6 mm particle size.

Flow rate: 0.9 mL min⁻¹; injection volume: 5 µL; retention times are given in minutes. ESI spectra were recorded on a Micro mass Quattro LC using ESI+ software with capillary voltage 3.98 kV and ESI mode positive ion trap detector. High-resolution mass spectra (HRMS) were recorded on a QSTAR XL Hybrid MS-MS mass spectrometer. Melting points were determined with an Electro thermal melting point apparatus and are uncorrected.

5.2. Synthetic Methods: Synthesis of (E)-1-substitutedphenyl-3-(3-(3,4,5-trimethoxyphenyl)-1H-pyrazol-5-yl)prop-2-en-1-one (13a-j):

The different pyrazole carbaldehydes (**12a-d**) used in this study were taken from our previous report.^[45]

To the 3-(3,4,5-trimethoxyphenyl)-1H-pyrazole-5-carbaldehyde (**12a**) prepared in the previous step was added corresponding substituted acetophenones and catalytic amount of sodium hydroxide in ethanol. The reaction mixture was stirred at room temperature for 3-4 h and progress of the reaction was monitored by TLC. After completion, ethanol was evaporated under vacuum and the residue was neutralized with dilute HCl solution. Finally the chalcones were extracted with ethyl acetate followed by purification was done by using column chromatography to obtain pure compounds of **13a-j** with good yields (70-85%).

5.2.1. (E)-1-phenyl-3-(3-(3,4,5-trimethoxyphenyl)-1H-pyrazol-5-yl)prop-2-en-1-one (13a):

This compound was prepared employing the above procedure by the addition of 3-(3,4,5-trimethoxyphenyl)-1H-pyrazole-5-carbaldehyde (**12a**) (262 mg 1.0 mmol) and acetophenone (120 mg 1.0 mmol). The compound obtained as brown colored solid Yield: 265 mg (73%); mp: 190-192 °C; ¹H NMR (300 MHz, DMSO-d₆); δ 3.89 (s, 9H, -OCH₃), 6.85 (s, 1H, ArH), 6.92 (s, 2H, ArH), 7.46 (m, 2H, *J*₁ = 7.4 Hz, ArH), 7.52-7.62 (m, 2H, ArH, -transH, *J* = 15.7 Hz), 7.7 (d, 1H, *J* = 15.8 Hz, -transH), 7.98 (d, 2H, *J* = 7.7 Hz, ArH); ¹³C NMR (75 MHz, DMSO-d₆); δ 55.9, 60.8, 123.0, 126.0, 128.4, 128.6, 132.7, 133.0, 137.4, 138.3, 144.9, 149.1, 153.1, 189.8 ppm; IR (KBr) (ν_{max}/cm⁻¹): ν = 3230, 2927, 1681, 1590, 1506, 1472, 1424, 1348, 1281, 1242, 1189, 1125, 1089 cm⁻¹; MS (ESI) *m/z* 365[M+H]; HR-MS (ESI) *m/z* for C₂₁H₂₁N₂O₄ calculated *m/z*: 365.1501, found *m/z*: 365.1499. Purity (HPLC): 97.80%.

5.2.2. (E)-1-(4-methoxyphenyl)-3-(3-(3,4,5-trimethoxyphenyl)-1H-pyrazol-5-yl)prop-2-en-1-one (13b):

This compound was prepared employing the above described procedure by the addition of **12a** (262 mg 1.0 mmol) and 1-(4-methoxyphenyl)ethanone (150 mg 1.0 mmol). Yellow colored solid

Yield: 248 mg (63%); mp: 189-191 °C; ^1H NMR (300 MHz, $\text{CDCl}_3+\text{DMSO-d}_6$); δ 3.89 (s, 6H, - OCH_3), 3.91 (s, 6H, - OCH_3) 6.87 (s, 1H, ArH), 6.91-7.01 (m, 4H, ArH), 7.58 (m, 2H, $J = 15.8$ Hz, transH), 8.02 (d, 2H, $J = 9.0$ Hz, ArH); ^{13}C NMR (75 MHz, DMSO-d_6): δ 54.1, 55.5, 59.9, 102.3, 113.3, 121.7, 130.1, 152.8, 162.8, 187.1 ppm; IR (KBr) ($\nu_{\text{max}}/\text{cm}^{-1}$): $\nu = 3245, 3004, 2932, 2834, 1659, 1588, 15557, 1515, 1476, 1457, 1424, 1390, 1337, 1312, 1230, 1182, 1127, \text{cm}^{-1}$; MS (ESI) m/z 395[M+H]; HR-MS (ESI) m/z for $\text{C}_{22}\text{H}_{23}\text{N}_2\text{O}_5$ calculated m/z : 395.1601, found m/z : 395.1599. Purity (HPLC): 97.64%.

5.2.3. (*E*)-1-(3,4-dimethoxyphenyl)-3-(3-(3,4,5-trimethoxyphenyl)-1H-pyrazol-5-yl)prop-2-en-1-one (**13c**):

This compound was prepared using the procedure described above by the addition of **12a** (262 mg 1.0 mmol) and 1-(3,4-dimethoxyphenyl)ethanone (180 mg 1.0 mmol). Pale yellow colored solid, yield: 275.8 mg (65%); mp: 176-177 °C; ^1H NMR (300 MHz, DMSO-d_6); δ 3.70 (s, 3H, - OCH_3), 3.87 (s, 12H, - OCH_3), 7.12-7.16 (m, 3H, ArH), 7.39 (d, 1H, $J = 14.9$ Hz, transH), 7.54-7.69 (m, 2H, ArH), 7.77-7.89 (m, 1H, ArH), 7.92 (d, 1H, $J = 15.8$ Hz, trasH); ^{13}C NMR (75 MHz, DMSO-d_6): δ 55.5, 55.7, 55.8, 55.9, 60.0, 101.6, 102.7, 103.6, 110.5, 110.8, 122.1, 123.0, 124.2, 129.0, 130.1, 130.3, 135.7, 137.5, 140.2, 143.5, 149.2, 151.4, 153.0, 186.7 ppm; IR (KBr) ($\nu_{\text{max}}/\text{cm}^{-1}$): $\nu = 3273, 2934, 2836, 1644, 1592, 1568, 1509, 1470, 1421, 1331, 1266, 1198, 1156, 1016, 915 \text{ cm}^{-1}$; MS (ESI) m/z 425 [M+H]; HR-MS (ESI) m/z for $\text{C}_{23}\text{H}_{25}\text{O}_6\text{N}_2$ calculated m/z : 425.1707, found m/z : 425.1696. Purity (HPLC): 98.31%.

5.2.4. (*E*)-1-(3,4,5-trimethoxyphenyl)-3-(3-(3,4,5-trimethoxyphenyl)-1H-pyrazol-5-yl)prop-2-en-1-one (**13d**):

This compound was prepared using the procedure described above by the addition of **12a** (262 mg 1.0 mmol) and 1-(3,4,5-trimethoxyphenyl)ethanone (210 mg 1.0 mmol). Yellow colored solid Yield: 263 mg (58%); mp: 208-210 °C; ^1H NMR (300MHz, DMSO-d_6); δ 3.78-3.99 (m, 18H, - OCH_3), 6.85 (s, 1H, ArH), 6.90 (s, 2H, ArH), 7.19-7.40 (m, 3H, ArH), 7.55 (d, 1H, $J = 15.8$ Hz transH), 7.77 (d, 1H, $J = 15.8$ Hz, transH); ^{13}C NMR (75 MHz, DMSO-d_6): δ 55.9, 56.2, 60.0, 60.1, 102.7, 106.1, 122.1, 132.7, 152.8, 153.2, 166.8, 187.6 ppm; IR (KBr) ($\nu_{\text{max}}/\text{cm}^{-1}$): $\nu = 3281, 2938, 2834, 1662, 1584, 1504, 1464, 1413, 1338, 1235, 1189, 1126, 1000, \text{cm}^{-1}$; MS (ESI) m/z 455[M+H]; HR-MS (ESI) m/z for $\text{C}_{24}\text{H}_{27}\text{O}_7\text{N}_2$ calculated m/z : 455.1812, found m/z : 455.1810. Purity (HPLC): 97.10%.

5.2.5. *(E)-1-(benzo[d][1,3]dioxol-5-yl)-3-(3-(3,4,5-trimethoxyphenyl)-1H-pyrazol-5-yl)prop-2-en-1-one (13e):*

This compound was prepared using the procedure described above by the addition of **12a** (262 mg 1.0 mmol) and 1-(benzo[d][1,3]dioxol-5-yl)ethanone (164 mg 1.0 mmol). Brown red colored solid Yield: 277.4 mg (68%); mp: 218-220 °C; ¹H NMR (300MHz, DMSO-d₆); δ 3.81 (s, 3H, -OCH₃), 3.81 (s, 6H, -OCH₃), 6.13 (s, 2H, OCH₂O), 6.95 (dd, 1H, *J* = 8.1 Hz, ArH), 6.99 (d, 1H, *J* = 13.7 Hz, transH), 7.01-7.09 (m, 1H, ArH), 7.50-7.56 (m, 1H, ArH) 7.66-7.79 (m, 2H, *J* = 16.8 Hz, transH, ArH), 7.81-7.91 (m, 1H, ArH), 13.27 (brs, 1H, NH); ¹³C NMR (75 MHz, DMSO-d₆); δ 55.3, 59.9, 101.1, 102.0, 107.1, 107.4, 121.3, 123.9, 131.8, 147.4, 150.9, 152.6, 186.8 ppm; IR (KBr) (ν_{max}/cm⁻¹): ν = 3420, 3239, 2928, 1657, 1578, 1508, 1457, 1385, 1314, 1243, 1126, 1035, 993 cm⁻¹; MS (ESI) *m/z* 409[M+H]; HR-MS (ESI) *m/z* for C₂₃H₂₂O₆N₂ calculated *m/z*: 409.1394, found *m/z*: 409.1388. Purity (HPLC): 97.67%.

5.2.6. *(E)-1-(3-fluoro-4-methoxyphenyl)-3-(3-(3,4,5-trimethoxyphenyl)-1H-pyrazol-5-yl)prop-2-en-1-one (13f):*

This compound was prepared using the procedure described above by the addition of **12a** (262 mg 1.0 mmol) and 1-(3-fluoro-4-methoxyphenyl)ethanone (168 mg 1.0 mmol). The compound obtained as yellow colored crystal Yield: 267.8 mg (67.8%); mp: 198-200 °C; ¹H NMR (400MHz, DMSO-d₆); δ 3.86 (s, 3H, -OCH₃), 3.96 (s, 6H, -OCH₃), 4.0 (s, 3H, -OCH₃), 6.89 (s, 1H, ArH), 7.04-7.07 (m, 1H, ArH), 7.12 (d, 1H, *J* = 8.4 Hz, ArH), 7.49-7.57 (m, 2H, ArH), 7.67-7.97 (m, 3H, *J* = 15.8 Hz, *J* = 8.3 Hz, transH, ArH); ¹³C NMR (75 MHz, DMSO-d₆); δ 55.0, 54.9, 59.3, 101.6, 11.5, 114.5, 114.7, 120.4, 124.6, 129.8, 148.9, 150.5, 152.1, 184.8, 185.6 ppm; IR (KBr) (ν_{max}/cm⁻¹): ν = 3329, 2937, 1680, 1587, 1503, 1467, 1421, 1240, 1128, 1030, 1002, 830 cm⁻¹; MS (ESI) *m/z* 413[M+H]; HR-MS (ESI) *m/z* for C₂₃H₂₂FO₅N₂ calculated *m/z*: 413.1497, found *m/z*: 413.1498. Purity (HPLC): 96.91%.

5.2.7. *(E)-1-(4-chlorophenyl)-3-(3-(3,4,5-trimethoxyphenyl)-1H-pyrazol-5-yl)prop-2-en-1-one (13g):*

This compound was prepared using the procedure described above by the addition of **12a** (262 mg 1.0 mmol) and 1-(4-chlorophenyl)ethanone (154 mg 1.0 mmol). The compound obtained as brown colored solid Yield: 260 mg (65.1%); mp: 208-210 °C; ¹H NMR (300 MHz, DMSO-d₆); δ 3.8-3.95 (m, 9H, -OCH₃), 6.83 (s, 1H, ArH), 6.89 (d, 1H, *J* = 15.0 Hz, transH), 6.94 (d, 1H, ArH), 7.32-7.54 (m, 3H, *J* = 16.0 Hz, ArH, transH), 7.01-8.04 (m, 3H, ArH); ¹³C NMR (75

MHz, DMSO- d_6): δ 55.4, 60.0, 99.5, 102.1, 134.5, 138.1, 138.6, 152.6, 196.6 ppm; IR (KBr) ($\nu_{\max}/\text{cm}^{-1}$): ν = 3322, 2933, 1731, 1682, 1589, 1502, 1466, 1402, 1363, 1237, 1125, 1090, 1001 cm^{-1} ; MS (ESI) m/z 399 [M+H]; HR-MS (ESI) m/z for $\text{C}_{21}\text{H}_{20}\text{ClO}_4\text{N}_2$ calculated m/z : 399.1106, found m/z : 399.1105. Purity (HPLC): 97.42%.

5.2.8. *(E)-1-(3,4-dichlorophenyl)-3-(3-(3,4,5-trimethoxyphenyl)-1H-pyrazol-5-yl)prop-2-en-1-one (13h)*:

This compound was prepared using the procedure described above by the addition of **12a** (262 mg 1.0 mmol) and 1-(3,4-dichlorophenyl)ethanone (189 mg 1.0 mmol). Yellow colored solid Yield: 280 mg (65%); mp: 203-205 °C; ^1H NMR (300 MHz, DMSO- d_6): δ 3.85 (s, 3H, -OCH₃), 3.94 (s, 3H, -OCH₃), 3.99 (s, 3H, -OCH₃), 6.90 (s, 1H, ArH), 7.03-7.07 (m, 1H, ArH), 7.12 (dd, 1H, J = 8.4 Hz, ArH), 7.53 (s, 1H, ArH), 7.67 (d, 1H, J = 14.16 Hz, transH), 7.76 (d, 1H, J = 15.4 Hz, transH), 7.84 (dd, 1H, J = 8.4 Hz, ArH), 7.92 (dd, 1H, J = 8.8 Hz, ArH); ^{13}C NMR (75 MHz, DMSO- d_6): δ 55.53, 60.03, 102.19, 112.08, 115.19, 115.44, 121.01, 125.35, 130.42, 137.18, 151.01, 152.78, 186.42 ppm; IR (KBr) ($\nu_{\max}/\text{cm}^{-1}$): ν = 3315, 2930, 2886, 1665, 1623, 1545, 1506, 1474, 1444, 1315, 1296, 1236, 1145, 1103, 1087, 1015 cm^{-1} ; MS (ESI) m/z 434 [M+H]; HR-MS (ESI) m/z for $\text{C}_{21}\text{H}_{19}\text{O}_4\text{N}_2\text{Cl}_2$ calculated m/z : 434.0643, found m/z : 434.0644. Purity (HPLC): 97.00%.

5.2.9. *(E)-1-(3,4-difluorophenyl)-3-(3-(3,4,5-trimethoxyphenyl)-1H-pyrazol-5-yl)prop-2-en-1-one (13i)*:

This compound was prepared using the procedure described above by the addition of **12a** (262 mg 1.0 mmol) and 1-(3,4-difluorophenyl)ethanone (156 mg 1.0 mmol). Yellow colored solid, yield: 240 mg (59.9%); mp: 191-193 °C; ^1H NMR (500 MHz, DMSO- d_6): δ 3.84 (s, 9H, -OCH₃), 5.90 (s, 1H, ArH), 6.19 (s, 1H, ArH), 6.50-6.52 (m, 1H, ArH), 6.85-7.05 (m, 2H, J = 8.3 Hz, J = 16.0 Hz, transH, ArH), 7.10 (d, 1H, J = 8.4 Hz, ArH), 7.35-7.56 (m, 2H J = 8.3 Hz, J = 16.5 Hz, transH, ArH); ^{13}C NMR (75 MHz, DMSO- d_6): δ 54.4, 55.1, 59.7, 100.0, 101.8, 113.4, 113.6, 115.6, 115.8, 116.6, 120.0, 120.2, 124.4, 134.5, 136.6, 141.6, 144.3, 152.3, 187.5 ppm; IR (KBr) ($\nu_{\max}/\text{cm}^{-1}$): ν = 3345, 2925, 2853, 1659, 1608, 1516, 1468, 1425, 1282, 1741, 1127, 1159, 1039 cm^{-1} ; MS (ESI) m/z 401[M+H]; HR-MS (ESI) m/z for $\text{C}_{21}\text{H}_{19}\text{O}_4\text{N}_2\text{F}_2$ calculated m/z : 401.1307, found m/z : 401.1322. Purity (HPLC): 97.89%.

5.2.10. *(E)*-1-(4-aminophenyl)-3-(3-(3,4,5-trimethoxyphenyl)-1*H*-pyrazol-5-yl)prop-2-en-1-one (**13j**):

This compound was prepared using the procedure described above by the addition of **12a** (262 mg 1.0 mmol) and 1-(4-aminophenyl)ethanone (135 mg 1.0 mmol). Yellow colored solid, yield: 280 mg (73.8%); mp: 197-199 °C; ¹H NMR (500 MHz, DMSO-d₆); δ 3.78 (s, 3H, -OCH₃), 3.86 (s, 6H, -OCH₃), 4.74 (brs, 1H, -NH₂), 6.62 (d, 2H, *J* = 8.4Hz, ArH), 6.73-6.75 (m, 1H, ArH), 6.97 (s, 2H, ArH), 7.58 (d, 1H, *J* = 15.6Hz, transH), 7.64 (d, 1H, *J* = 15.6 Hz, transH), 7.85 (dd, 2H, *J* = 8.6 Hz, ArH); ¹³C NMR (75 MHz, DMSO-d₆); δ 55.2, 59.8, 101.4, 101.8, 112.5, 121.8, 125.8, 130.1, 136.7, 152.4, 152.0, 186.1 ppm; IR (KBr) (ν_{max}/cm⁻¹): ν = 3448, 3368, 3243, 2923, 2853, 1729, 1647, 1584, 1461, 1338, 1310, 1274, 1227, 1172, 1119, 1025, 981 cm⁻¹; MS (ESI) *m/z* 380 [M+H]; HR-MS (ESI) *m/z* for C₂₁H₂₂O₄ N₃ calculated *m/z*: 380.1606, found *m/z*: 380.1605. Purity (HPLC): 97.47%.

5.3. Synthesis of *(E)*-3-(3-(benzo[d][1,3]dioxol-5-yl)-1*H*-pyrazol-5-yl)-1-substitutedphenylprop-2-en-1-one **14(a-j)**:

To the 3-(benzo[d][1,3]dioxol-5-yl)-1*H*-pyrazole-5-carbaldehyde (**12b**) prepared in the previous step was added corresponding substituted acetophenones and catalytic amount of sodium hydroxide in ethanol. The reaction mixture was stirred at room temperature for 3-4 h and progress of the reaction was monitored by TLC. After completion, ethanol was evaporated under vacuum and the residue was neutralised with dilute HCl solution. Finally the chalcones were extracted with ethyl acetate followed by purification was done by using column chromatography to obtain pure compounds of **14a-j** with good yields (60-75%).

5.3.1. *(E)*-3-(3-(benzo[d][1,3]dioxol-5-yl)-1*H*-pyrazol-5-yl)-1-phenylprop-2-en-1-one (**14a**):

This compound was prepared using the procedure described above by the addition of 3-(benzo[d][1,3]dioxol-5-yl)-1*H*-pyrazole-5-carbaldehyde **12b** (216 mg 1.0 mmol) and acetophenone (120 mg 1.0 mmol). Brown colored solid, yield: 245 mg (76%); mp: 190-192 °C; ¹H NMR (300MHz, DMSO-d₆); δ 6.03 (s, 2H, -OCH₂O-), 6.87 (d, 1H, *J* = 7.9 Hz, ArH), 6.93 (s, 1H, ArH), 7.25-7.33 (m, 2H, ArH), 7.53 (d, 1H, *J* = 12.8 Hz, transH), 7.52-7.54 (m, 1H, ArH), 7.58 (d, 1H, *J* = 14.8 Hz, transH), 7.69-7.72 (m, 2H, ArH), 8.06 (d, 2H, *J* = 7.1 Hz, ArH); ¹³C NMR (75 MHz, DMSO-d₆); δ 100.1, 101.4, 104.9, 107.5, 118.2, 121.2, 127.3, 127.6, 131.8, 133.0, 136.8, 146.4, 146.9, 188.7 ppm; IR (KBr) (ν_{max}/cm⁻¹): ν = 3296, 3120, 2996, 1690, 1638, 1596, 1541, 1436, 1412, 1396, 1311, 1274, 1156, 1100, 1026 cm⁻¹; MS (ESI) *m/z* 319 [M+H];

HR-MS (ESI) m/z for $C_{19}H_{15}N_2O_3$ calculated m/z : 319.1004, found m/z : 319.1003. Purity (HPLC): 96.32%.

5.3.2. (*E*)-3-(3-(benzo[d][1,3]dioxol-5-yl)-1H-pyrazol-5-yl)-1-(4-methoxyphenyl)prop-2-en-1-one (**14b**):

This compound was prepared using the procedure described above by the addition of **12b** (216 mg 1.0 mmol) and 1-(4-methoxyphenyl)ethanone (150 mg 1.0 mmol). Yellow colored solid, yield: 265 mg (76.1%); mp: 196-198 °C; 1H NMR (300 MHz, DMSO- d_6): δ 3.98 (s, 3H, -OCH₃), 6.00 (s, 2H, -OCH₂O-), 6.77 (d, 1H, J = 8.6 Hz, ArH), 6.87 (m, 1H, J = 8.5 Hz, ArH), 7.01 (m, 1H, J = 8.6 Hz, ArH), 7.24-7.32 (m, 1H, ArH) 7.35 (d, 2H, J = 7.7 Hz, ArH) 7.65 (d, 1H, J = 16.7 Hz, transH), 7.76 (d, 1H, J = 15.8 Hz, transH), 8.08 (m, 2H, J = 8.5 Hz, ArH); ^{13}C NMR (75 MHz, DMSO- d_6): δ 54.0, 99.7, 104.4, 107.0, 112.4, 117.7, 120.7, 129.2, 145.9, 146.5, 161.9, 186.9 ppm; IR (KBr) (ν_{max}/cm^{-1}): ν = 3237, 2909, 1659, 1608, 1587, 1549, 1503, 1470, 1342, 1294, 1256, 1226, 1174, 1037 cm^{-1} ; MS (ESI) m/z 349 [M+H]; HR-MS (ESI) m/z for $C_{20}H_{17}O_4N_2$ calculated m/z : 349.1195, found m/z : 349.1194. Purity (HPLC): 97.50%.

5.3.3. (*E*)-3-(3-(benzo[d][1,3]dioxol-5-yl)-1H-pyrazol-5-yl)-1-(3,4-dimethoxyphenyl)prop-2-en-1-one (**14c**):

This compound was prepared using the procedure described above by the addition of **12b** (216 mg 1.0 mmol) and 1-(3,4-dimethoxyphenyl)ethanone (180 mg 1.0 mmol). Pale yellow colored solid, yield: 285 mg (75.3%); mp: 190-192 °C; 1H NMR (300 MHz, DMSO- d_6): δ 3.95 (s, 3H, -OCH₃), 3.97 (s, 3H, -OCH₃), 6.02 (s, 2H, OCH₂O), 6.83-7.06 (m, 3H, J = 16.4 Hz, transH, ArH), 7.29 (d, 2H, J = 8.1 Hz, ArH), 7.60-7.73 (m, 2H, J = 14.8 Hz, transH, ArH), 7.78 (d, 1H, J = 6.8 Hz, ArH) 7.82 (s, 1H, ArH); ^{13}C NMR (75 MHz, DMSO- d_6): δ 54.0, 54.2, 99.4, 104.1, 106.7, 108.8, 109.0, 117.3, 120.2, 121.4, 145.6, 146.2, 147.2, 151.8, 185.6 ppm; IR (KBr) (ν_{max}/cm^{-1}): ν = 3274, 2923, 2852, 1654, 1598, 1573, 1501, 1457, 1419, 1394, 1346, 1297, 1272, 1236, 1167, 1031 cm^{-1} ; MS (ESI) m/z 379[M+H]; HR-MS (ESI) m/z for $C_{21}H_{19}O_5N_2$ calculated m/z : 379.1289, found m/z : 379.2900. Purity (HPLC): 98.11%.

5.3.4. (*E*)-3-(3-(benzo[d][1,3]dioxol-5-yl)-1H-pyrazol-5-yl)-1-(3,4,5-trimethoxyphenyl)prop-2-en-1-one (**14d**):

This compound was prepared using the procedure described above by the addition of **12b** (216 mg 1.0 mmol) and 1-(3,4,5-trimethoxyphenyl)ethanone (210 mg 1.0 mmol). Pale yellow colored solid, yield: 270 mg (66%); mp: 208-210 °C; 1H NMR (300MHz, DMSO- d_6): δ 3.90 (s, 3H, -

OCH₃), 3.96 (s, 6H, -OCH₃), 6.01 (s, 2H, -OCH₂O-), 6.82-6.92 (m, 2H, ArH), 7.27-7.37 (m, 4H, *J* = 17.0 Hz, transH, ArH), 7.66-7.67 (m, 2H, *J* = 16.0 Hz, transHArH); ¹³C NMR (75 MHz, DMSO-d₆): δ 55.6, 60.0, 100.4, 102.0, 105.3, 107.8, 118.6, 121.1, 124.8, 141.6, 146.7, 147.2, 152.3, 197.8 ppm; IR (KBr) (ν_{max}/cm⁻¹): ν = 3255, 3156, 2924, 1653, 1574, 1499, 1464, 1415, 1335, 1270, 1239, 1159, 1125, 1044, 1004 cm⁻¹; MS (ESI) *m/z* 409[M+H]; HR-MS (ESI) *m/z* for C₂₂H₂₁O₆N₂ calculated *m/z*: 409.1403, found *m/z*: 409.1402. Purity (HPLC): 97.68%.

5.3.5. (*E*)-1-(benzo[d][1,3]dioxol-5-yl)-3-(3-(benzo[d][1,3]dioxol-5-yl)-1H-pyrazol-5-yl)prop-2-en-1-one (**14e**):

This compound was prepared using the procedure described above by the addition of **12b** (216 mg 1.0 mmol) and 1-(benzo[d][1,3]dioxol-5-yl)ethanone (164 mg 1.0 mmol). Brown red colored solid, yield: 280 mg (77.3%); mp: 218-220 °C; ¹H NMR (300MHz, DMSO-d₆): δ 6.03 (s, 2H, -OCH₂O-), 6.13 (s, 2H, -OCH₂O-), 6.89 (d, *J* = 7.9 Hz, 1H, ArH), 6.97 (s, 1H, ArH), 7.02 (d, 1H, *J* = 12.6 Hz, TransH), 7.24-7.36 (d, 1H, *J* = 12.6 Hz, transH) 7.56 (s, 1H, ArH), 7.62 (d, 1H, *J* = 8.0 Hz, ArH), 7.69-7.80 (m, 2H, ArH), 8.02-8.05 (m, 1H, ArH); ¹³C NMR (75 MHz, DMSO-d₆): δ 99.3, 100.2, 103.8, 106.0, 106.1, 106.7, 117.1, 120.2, 122.9, 130.4, 145.4, 146.0, 146.3, 149.8, 184.9 ppm; IR (KBr) (ν_{max}/cm⁻¹): ν = 3252, 2921, 2852, 1659, 1606, 1585, 1555, 1500, 1468, 1346, 1289, 1115, 1036, 972 cm⁻¹; MS (ESI) *m/z* 363[M+H]; HR-MS (ESI) *m/z* for C₂₀H₁₅O₅N₂ calculated *m/z*: 363.0990, found *m/z*: 363.0988. Purity (HPLC): 96.58%.

5.3.6. (*E*)-3-(3-(benzo[d][1,3]dioxol-5-yl)-1H-pyrazol-5-yl)-1-(3-fluoro-4-methoxyphenyl)prop-2-en-1-one (**14f**):

This compound was prepared using the procedure described above by the addition of **12b** (216 mg 1.0 mmol) and 1-(3-fluoro-4-methoxyphenyl)ethanone (168 mg 1.0 mmol). Yellow colored crystal Yield: 260 mg (71%); mp: 199-200 °C; ¹H NMR (400MHz, DMSO-d₆): δ 3.99 (s, 3H, -OCH₃), 6.02 (s, 2H, -OCH₂O), 6.87 (dd, 1H, *J*= 11.1 Hz, ArH), 7.07 (d, 1H, *J*= 16.8 Hz, transH), 7.25-7.35 (m, 1H, ArH), 7.63 (s, 5H, ArH), 7.88 (d, 1H, *J*= 16.8 Hz, transH); ¹³C NMR (75 MHz, DMSO-d₆): δ 54.7, 99.6, 104.3, 106.9, 111.3, 117.2, 117.6, 120.0, 124.4, 129.2, 145.8, 146.4, 151.1, 185.1 ppm; IR (KBr) (ν_{max}/cm⁻¹): ν = 3242, 2922, 2851, 1661, 1607, 1516, 1465, 1276, 1239, 1139, 1037, 970, 930 cm⁻¹; MS (ESI) *m/z* 367 [M+H]; HR-MS (ESI) *m/z* 367 for C₂₀H₁₆O₄N₂F calculated *m/z*: 367.1099, found *m/z*: 367.1090. Purity (HPLC): 97.80%.

5.3.7. (*E*)-3-(3-(benzo[d][1,3]dioxol-5-yl)-1H-pyrazol-5-yl)-1-(4-chlorophenyl)prop-2-en-1-one (**14g**):

This compound was prepared using the procedure described above by the addition of **12b** (216 mg 1.0 mmol) and 1-(4-chlorophenyl)ethanone (154 mg 1.0 mmol). Brown colored solid, yield: 240 mg (68%); mp: 209-211 °C; ¹H NMR (300 MHz, DMSO-d₆); δ 5.97 (s, 2H, -OCH₂O-), 6.29 (s, 1H, ArH), 6.81 (d, 1H, *J* = 16.8 Hz, transH), 7.10-7.15 (d, 1H, *J* = 16.0 Hz, transH), 7.26 (s, 1H, ArH) 7.42 (d, 3H, *J* = 7.9 Hz, ArH), 7.90 (d, 3H, *J* = 8.9 Hz, ArH); IR (KBr) (ν_{max}/cm⁻¹): ν = 3421, 2899, 1682, 1589, 1492, 1463, 1401, 1360, 1239, 1093, 1038, 1012, 983 cm⁻¹; MS (ESI) *m/z* 353 [M+H]; HR-MS (ESI) *m/z* for C₁₉H₁₄O₃N₂Cl calculated *m/z*: 353.1448, found *m/z*: 353.1448. Purity (HPLC): 95.85%.

5.3.8. (*E*)-3-(3-(benzo[*d*][1,3]dioxol-5-yl)-1*H*-pyrazol-5-yl)-1-(3,4-dichlorophenyl)prop-2-en-1-one (**14h**):

This compound was prepared using the procedure described above by the addition of **12b** (216 mg 1.0 mmol) and 1-(3,4-dichlorophenyl)ethanone (189 mg 1.0 mmol). Yellow colored solid Yield: 182 mg (80%); mp: 196-198 °C; ¹H NMR (300 MHz, DMSO-d₆); δ 6.06 (s, 2H, -OCH₂O-), 6.84-6.88 (m, 1H, ArH), 6.88-6.95 (m, 1H, ArH), 6.98 (d, 1H, *J* = 16.0 Hz, transH), 6.08-6.18 (m, 1H, ArH) 7.22 (d, 1H, *J* = 7.9 Hz, ArH), 7.40 (d, 1H, *J* = 16.1 Hz, transH), 7.57-7.66 (m, 1H, ArH), 7.82 (m, 2H, ArH); ¹³C NMR (75 MHz, DMSO-d₆): δ ppm; IR (KBr) (ν_{max}/cm⁻¹): ν = 3149, 3120, 2939, 2845, 1687, 1589, 1529, 1513, 1436, 1354, 1285, 1196, 1235, 1065 cm⁻¹; MS (ESI) *m/z* 388 [M+H]; HR-MS (ESI) *m/z* for C₁₉H₁₃O₃N₂Cl₂ calculated *m/z*: 388.0195, found *m/z*: 388.0196. Purity (HPLC): 96.94%.

5.3.9. (*E*)-1-(3,4-difluorophenyl)-3-(3-(3,4,5-trimethoxyphenyl)-1*H*-pyrazol-5-yl)prop-2-en-1-one (**14i**):

This compound was prepared using the procedure described above by the addition of **12b** (216 mg 1.0 mmol) and 1-(3,4-difluorophenyl)ethanone (156 mg 1.0 mmol). Yellow colored solid, yield: 193 mg (77%); mp: 198-199 °C; ¹H NMR (500 MHz, DMSO-d₆); δ 6.01 (s, 2H, -OCH₂O-), 6.86 (d, 1H, *J* = 7.9 Hz, ArH), 6.91 (s, 1H, ArH), 7.07-7.18 (m, 1H, ArH), 7.20-7.32 (m, 1H, ArH), 7.68-7.72 (m, 2H, ArH), 7.80 (s, 1H, ArH), 7.84 (d, 1H, *J* = 12.2 Hz, transH), 7.89 (d, 1H, *J* = 16.0 Hz, transH); ¹³C NMR (75 MHz, DMSO-d₆): δ 100.8, 105.5, 108.3, 115.1, 116.7, 116.9, 118.8, 121.7, 136.0, 143.6, 146.9, 147.6, 163.6, 191.5 ppm; IR (KBr) (ν_{max}/cm⁻¹): ν = 3120, 3066, 3011, 2856, 1638, 1620, 1545, 1496, 1491, 1432, 1379, 1246 cm⁻¹; MS (ESI) *m/z* 355 [M+H]; HR-MS (ESI) *m/z* for C₁₉H₁₃O₃N₂F₂ calculated *m/z*: 355.0816, found *m/z*: 355.0816. Purity (HPLC): 97.66%.

5.3.10. *(E)*-1-(4-aminophenyl)-3-(3-(benzo[d][1,3]dioxol-5-yl)-1H-pyrazol-5-yl)prop-2-en-1-one (**14j**):

This compound was prepared using the procedure described above by the addition of **12b** (216 mg 1.0 mmol) and 1-(4-aminophenyl)ethanone (135 mg 1.0 mmol). Yellow colored solid, yield: 280 mg (84%); mp: 185-187 °C; ¹H NMR (500 MHz, DMSO-d₆): δ 5.51 (brs, 2H, -NH₂), 6.02 (s, 2H, -OCH₂O-), 6.69 (d, 2H, *J* = 8.6 Hz, ArH), 6.8-6.94 (m, 2H, ArH), 7.24-7.36 (m, 2H, ArH), 7.60 (d, 1H, *J* = 15.8 Hz, transH), 7.70 (d, 1H, *J* = 15.8 Hz, transH), 7.81 (s, 1H ArH), 7.88 (d, 1H, *J* = 8.6 Hz, ArH); ¹³C NMR (75 MHz, DMSO-d₆): δ 55.2, 59.8, 101.4, 101.8, 112.5, 121.8, 125.8, 130.1, 136.7, 152.0, 186.1 ppm; IR (KBr) (ν_{max}/cm⁻¹): ν = 3155, 2926, 1650, 1550, 1466, 1460, 1410, 1365, 1280, 1250, 1180, 1125, 1100, 1065, 985 cm⁻¹; MS (ESI) *m/z* 334 [M+H]; HR-MS (ESI) *m/z* for C₁₉H₁₆O₃N₃ calculated *m/z*: 334.1190, found *m/z*: 334.1190. Purity (HPLC): 96.85%.

5.4. Synthesis of *(E)*-1-(substitutedphenyl)-3-(3-(substitutedphenyl)-1H-pyrazol-5-yl)prop-2-en-1-one (**15-16a-d**)

To the 3-substitutedphenyl-1H-pyrazole-5-carbaldehydes (**12c&d**) prepared in the previous step was added corresponding substituted acetophenones and catalytic amount of sodium hydroxide in ethanol. The reaction mixture was stirred at room temperature for 3-4 h and progress of the reaction was monitored by TLC. After completion, ethanol was evaporated under vacuum and the residue was neutralised with dilute HCl solution. Finally the chalcones were extracted with ethyl acetate followed by purification was done by using column chromatography to obtain pure compounds of **17a-j** with good yields (60-75%).

5.4.1. *(E)*-3-(3-(3,4-dimethoxyphenyl)-1H-pyrazol-5-yl)-1-(3,4,5-trimethoxyphenyl)prop-2-en-1-one (**15a**):

This compound was prepared using the procedure described above by the addition of 3-(3,4-dimethoxyphenyl)-1H-pyrazole-5-carbaldehyde **12c** (232 mg 1.0 mmol) and 1-(3,4,5-trimethoxyphenyl)ethanone (210 mg 1.0 mmol). Yellow colored solid, yield: 310 mg (73.1%); mp: 197-199 °C; ¹H NMR (400MHz, DMSO-d₆): δ 3.92 (s, 3H, -OCH₃), 3.93 (s, 3H, -OCH₃), 3.97 (s, 6H, -OCH₃), 6.86 (s, 1H, ArH), 6.94 (d, 1H, *J* = 8.3 Hz, ArH), 7.31-7.42 (m, 3H, ArH), 7.42-7.53 (m, 1H, ArH) 7.65 (d, 1H, *J* = 15.8 Hz, transH) 7.79 (d, 1H, *J* = 15.8 Hz, transH); ¹³C NMR (75 MHz, DMSO-d₆): δ 54.4, 54.9, 59.2, 101.0, 104.6, 105.3, 107.5, 110.2, 116.7, 120.4, 131.8, 140.8, 147.5, 147.6, 151.6, 186.7 ppm; IR (KBr) (ν_{max}/cm⁻¹): ν = 3253, 2923, 2852, 1735,

1687, 1654, 1568, 1509, 1464, 1411, 1388, 1337, 1250, 1225, 1184, 1155, 1118, 1065, 1019, 980 cm^{-1} ; MS (ESI) m/z 425 [M+H]; HR-MS (ESI) m/z for $\text{C}_{23}\text{H}_{25}\text{O}_6\text{N}_2$ calculated m/z : 425.1707, found m/z : 425.1699. Purity (HPLC): 98.79%.

5.4.2. *(E)-1-(3,4-dimethoxyphenyl)-3-(3-(3,4-dimethoxyphenyl)-1H-pyrazol-5-yl)prop-2-en-1-one (15b):*

This compound was prepared using the procedure described above by the addition of **12c** (232 mg 1.0 mmol) and 1-(3,4-dimethoxyphenyl)ethanone (180 mg 1.0 mmol). Yellow solid, yield: 300 mg (76.1%); mp: 208-210 °C; ^1H NMR (300MHz, DMSO-d_6); δ 3.82 (s, 3H, $-\text{OCH}_3$), 3.89 (s, 9H, $-\text{OCH}_3$), 6.73-7.00 (m, 3H, ArH), 7.21-7.41 (m, 2H, ArH), 7.42-7.54 (dd, 1H, $J = 13.5$ Hz, transH), 7.56-7.61 (s, 1H, ArH), 7.62-7.80 (m, 2H, $J = 14.9$ Hz, transH, ArH); ^{13}C NMR (75 MHz, DMSO-d_6); δ 55.2, 108.4, 109.9, 110.2, 111.1, 117.5, 121.3, 122.6, 130.3, 148.3, 148.4, 152.7, 186.9 ppm; IR (KBr) ($\nu_{\text{max}}/\text{cm}^{-1}$): $\nu = 3251, 2930, 2838, 1655, 1590, 1570, 1513, 1465, 1418, 1388, 1331, 1266, 1163, 1023, 968$ cm^{-1} ; MS (ESI) m/z 395 [M+H]; HR-MS (ESI) m/z for $\text{C}_{22}\text{H}_{23}\text{O}_5\text{N}_2$ calculated m/z : 395.1601, found m/z : 395.1599. Purity (HPLC): 97.45%.

5.4.3. *(E)-1-(benzo[d][1,3]dioxol-5-yl)-3-(3-(3,4-dimethoxyphenyl)-1H-pyrazol-5-yl)prop-2-en-1-one (15c):*

This compound was prepared using the procedure described above by the addition of **12c** (232 mg 1.0 mmol) and 1-(benzo[d][1,3]dioxol-5-yl)ethanone (164 mg 1.0 mmol). Yellow colored solid, yield: 285 mg (75.3%); mp: 196-197 °C; ^1H NMR (300 MHz, DMSO-d_6); δ 3.85 (s, 3H, $-\text{OCH}_3$), 3.89 (s, 3H, $-\text{OCH}_3$), 6.14 (s, 2H, $-\text{OCH}_2\text{O}-$), 6.77-7.22 (m, 3H, ArH), 7.27-7.48 (m, 2H, $J = 13.7$ Hz, transH, ArH), 7.57-7.71 (m, 2H, ArH), 7.75 (dd, 1H, $J = 8.1$ Hz, ArH), 8.12 (d, 1H, $J = 16.2$ Hz, transH); ^{13}C NMR (75 MHz, DMSO-d_6); δ 54.7, 100.7, 106.7, 106.9, 110.4, 116.9, 120.8, 123.5, 131.4, 147.0, 147.9, 150.5, 165.7, 186.2 ppm; IR (KBr) ($\nu_{\text{max}}/\text{cm}^{-1}$): $\nu = 3237, 2922, 2844, 1769, 1657, 1607, 1581, 1524, 1455, 1373, 1323, 1252, 1165, 1131, 1028, 971, 939$ cm^{-1} ; MS (ESI) m/z 379 [M+H]; HR-MS (ESI) m/z for $\text{C}_{21}\text{H}_{19}\text{O}_5\text{N}_2$ calculated m/z : 379.1285, found m/z : 379.1280. Purity (HPLC): 97.95%.

5.4.4. *(E)-1-(4-aminophenyl)-3-(3-(3,4-dimethoxyphenyl)-1H-pyrazol-5-yl)prop-2-en-1-one (15d):*

This compound was prepared using the procedure described above by the addition of **12c** (232 mg 1.0 mmol) and 1-(4-aminophenyl)ethanone (135 mg 1.0 mmol). Yellow solid Yield: 245 mg (70.2%); mp: 218-220 °C; ^1H NMR (400 MHz, DMSO-d_6); δ 3.91 (s, 3H, $-\text{OCH}_3$), 3.97 (s, 3H,

OCH₃), 4.93 (brs, 2H, NH₂), 6.71 (d, 2H, *J* = 8.4 Hz, ArH), 6.81 (s, 1H, ArH), 7.29-7.43 (m, 2H, ArH), 7.50 (s, 2H, ArH), 7.65 (d, 1H, *J* = 14.3 Hz, transH), 7.72 (d, 2H, *J* = 16.1 Hz, transH), 7.93 (d, 2H, *J* = 6.9 Hz, ArH); ¹³C NMR (75 MHz, DMSO-d₆): δ 54.5, 110.3, 107.7, 111.8, 116.7, 121.2, 124.7, 129.6, 147.5, 147.7, 152.0, 185.1 ppm; IR (KBr) (ν_{max}/cm⁻¹): ν = 3428, 3129, 3018, 2875, 1675, 1545, 1501, 1498, 1452, 1350, 1265, 1135, 1072, 945 cm⁻¹; MS (ESI) *m/z* 350 [M+H]; HR-MS (ESI) *m/z* for C₂₀H₂₀O₃N₃ calculated *m/z*: 350.1499, found *m/z*: 350.1504. Purity (HPLC): 97.19%.

5.4.5. (*E*)-3-(3-(4-methoxyphenyl)-1H-pyrazol-5-yl)-1-(3,4,5-trimethoxyphenyl)prop-2-en-1-one (**16a**):

This compound was prepared employing above procedure by the addition of 3-(4-methoxyphenyl)-1H-pyrazole-5-carbaldehyde **12d** (202 mg 1.0 mmol) and 1-(3,4,5-trimethoxyphenyl)ethanone (210 mg 1.0 mmol). Yellow solid, yield: 300 mg (75.9%); mp: 190-192 °C; ¹H NMR (500MHz, DMSO-d₆): δ 3.75 (s, 3H, -OCH₃), 3.80 (s, 3H, -OCH₃), 3.87 (s, 6H, -OCH₃), 6.81 (s, 1H, ArH), 6.86 (d, 1H, *J* = 8.4 Hz, ArH), 7.22-7.27 (s, 3H, ArH), 7.55-7.69 (m, 4H, *J* = 15.8 Hz, tranH, ArH); ¹³C NMR (75 MHz, DMSO-d₆): δ 55.1, 56.1, 60.1, 105.9, 114.2, 121.8, 126.5, 132.7, 152.8, 159.1, 175.2, 187.5 ppm; IR (KBr) (ν_{max}/cm⁻¹): ν = 3254, 3008, 2934, 2837, 1655, 1596, 1569, 1511, 1452, 1416, 1392, 1251, 1165, 1059, 964 cm⁻¹; MS (ESI) *m/z* 395 [M+H]; HR-MS (ESI) *m/z* for C₂₂H₂₃N₂O₅ calculated *m/z*: 395.1601, found *m/z*: 395.1607. Purity (HPLC): 96.81%.

5.4.6. (*E*)-1-(3,4-dimethoxyphenyl)-3-(3-(4-methoxyphenyl)-1H-pyrazol-5-yl)prop-2-en-1-one (**16b**):

This compound was prepared using the above procedure by the addition of **12d** (202 mg 1.0 mmol) and 1-(3,4-dimethoxyphenyl)ethanone (180 mg 1.0 mmol). Yellow solid, yield: 270 mg (74.1%); mp: 177-179 °C; ¹H NMR (300 MHz, DMSO-d₆): δ 3.76 (s, 3H, -OCH₃), 3.86 (s, 3H, -OCH₃), 3.87 (s, 3H, -OCH₃), 6.78-6.90 (m, 3H, ArH), 6.95 (d, 1H, *J* = 12.3 Hz, transH), 7.53 (s, 1H, ArH), 7.58-7.75 (m, 4H, *J* = 12.9 Hz, tranH, ArH), 7.83 (s, 1H, ArH); ¹³C NMR (75 MHz, DMSO-d₆): δ 54.7, 55.3, 55.4, 101.6, 110.1, 110.3, 113.7, 121.4, 122.7, 126.2, 130.3, 148.5, 152.8, 158.9, 186.9 ppm; IR (KBr) (ν_{max}/cm⁻¹): ν = 3260, 2957, 1581, 1600, 1346, 1370, 1244, 1438, 1821, 1340, 1169, 1306, 1215, 1189, 1040 cm⁻¹; MS (ESI) *m/z* 365 [M+H]; HR-MS (ESI) *m/z* for C₂₁H₂₁O₄N₂ calculated *m/z*: 365.1495, found *m/z*: 365.1489. Purity (HPLC): 98.59%.

5.4.7. *(E)*-1-(benzo[d][1,3]dioxol-5-yl)-3-(3-(4-methoxyphenyl)-1H-pyrazol-5-yl)prop-2-en-1-one (**16c**):

This compound was prepared using the above procedure by the addition of **12d** (202 mg 1.0 mmol) and 1-(benzo[d][1,3]dioxol-5-yl)ethanone (164 mg 1.0 mmol). Yellow colored solid, yield: 260 mg (74.7%); mp: 208-210 °C; ¹H NMR (300 MHz, DMSO-d₆); δ 3.82 (s, 3H, -OCH₃), 6.14 (s, 2H, -OCH₂O), 6.85-7.13 (m, 4H, *J* = 15.8 Hz, transH, ArH), 7.43-7.80 (m, 5H, *J* = 15.6 Hz, transH, ArH), 8.09 (s, 1H, ArH), 13.38 (brs, 1H, -NH); ¹³C NMR (75 MHz, DMSO-d₆); δ 54.3, 100.6, 107.6, 109.0, 109.4, 110.3, 116.5, 120.4, 121.3, 121.6, 129.3, 147.4, 147.6, 151.8, 186.0 ppm; IR (KBr) (ν_{max}/cm⁻¹): ν = 3236, 2928, 1676, 1628, 1577, 1542, 1502, 1476, 1342, 1320, 1296, 1265, 1140, 1020, 944 cm⁻¹; MS (ESI) *m/z* 349 [M+H]; HR-MS (ESI) *m/z* for C₂₀H₁₇O₄N₂ calculated *m/z*: 349.1195, found *m/z*: 349.1194. Purity (HPLC): 97.22%.

5.4.8. *(E)*-1-(4-aminophenyl)-3-(3-(4-methoxyphenyl)-1H-pyrazol-5-yl)prop-2-en-1-one (**16d**):

This compound was prepared using the procedure described above by the addition of **12d** (202 mg 1.0 mmol) and 1-(4-aminophenyl)ethanone (135 mg 1.0 mmol). Pale yellow colored solid Yield: 255 mg (79.9%); mp: 190-192 °C; ¹H NMR (300 MHz, DMSO-d₆); δ 3.84 (s, 3H, -OCH₃), 5.72 (brs, 2H, NH₂), 6.67 (d, 2H, *J* = 8.6 Hz, ArH), 6.80-7.01 (m, 3H, ArH), 7.65-7.76 (m, 3H, *J* = 13.6 Hz, transH, ArH), 7.82-8.02 (m, 3H, *J* = 13.4 Hz, transH, ArH); ¹³C NMR (75 MHz, DMSO-d₆); δ 53.8, 111.8, 112.7, 121.1, 124.8, 125.3, 129.5, 152.0, 157.1, 185.1 ppm; IR (KBr) (ν_{max}/cm⁻¹): ν = 3448, 3363, 3203, 3003, 2923, 1660, 1609, 1632, 1526, 1464, 1335, 1294, 1244, 1177 cm⁻¹; MS (ESI) *m/z* 320 [M+H]; HR-MS (ESI) *m/z* for C₁₉H₁₈O₂N₃ calculated *m/z*: 320.1398, found *m/z*: 320.1393. Purity (HPLC): 97.27%.

5.5. Synthesis of *(E)*-1-substitutedphenyl-3-(3-(3,4,5-trimethoxyphenyl)-1H-pyrazol-5-yl)prop-2-en-1-one **17(a-f)**

To the 3-(3,4,5-trimethoxyphenyl)-1H-pyrazole-5-carbaldehyde (**12a**) prepared in the above step was added different ketones and catalytic amount of sodium hydroxide (1.0 ml) in ethanol. The reaction mixture was heated to reflux for 1-2 h at 85 °C. Completion of the reaction was determined by TLC followed by extracted the crude compounds with ethyl acetate thrice and combined organic layers dried on anhydrous sodium sulphate. The crude compounds were purified by means of column chromatography using ethyl acetate and hexane as solvent system to provide pure compounds of **17a-f** in good yields.

5.5.1. *(E)*-4-(3-(3,4,5-trimethoxyphenyl)-1H-pyrazol-5-yl)but-3-en-2-one (**17a**):

This compound was prepared using the procedure described above by the addition of 3-(3,4,5-trimethoxyphenyl)-1*H*-pyrazole-5-carbaldehyde (**12a**) (262 mg 1.0 mmol) and propan-2-one (58 mg 1.0 mmol). Yellow colored solid, yield: 210 mg (69.4%); mp: 193-195 °C; ¹H NMR (500 MHz, DMSO-*d*₆); δ 2.35 (s, 3H, CH₃), 3.89 (s, 9H, -OCH₃), 6.71 (d, 1H, *J* = 16.4 Hz transH), 6.77 (s, 1H, ArH), 6.89 (s, 2H, ArH), 7.48 (d, 1H, *J* = 16.4 Hz transH); ¹³C NMR (75 MHz, DMSO-*d*₆); δ 41.9, 57.4, 58.6, 98.3, 99.6, 104.3, 107.0, 109.6, 117.5, 127.4, 128.2, 138.9, 146.4, 195.7 ppm; IR (KBr) ($\nu_{\max}/\text{cm}^{-1}$): ν = 3229, 3131, 2940, 2832, 1734, 1665, 1629, 1591, 1504, 1472, 1416, 1327, 1125, 1039 cm^{-1} ; MS (ESI) *m/z* 303 [M+H]; HR-MS (ESI) *m/z* for C₁₆H₁₉O₄N₂ calculated *m/z*: 303.1339, found *m/z*: 303.1339. Purity (HPLC): 97.80%.

5.5.2. (*E*)-2-((3-(3,4,5-trimethoxyphenyl)-1*H*-pyrazol-5-yl)methylene)cyclohexanone (**17b**):

This compound was prepared using the procedure described above by the addition of **12a** (262 mg 1.0 mmol) and cyclohexanone (98 mg 0.0659 mmol). Yellow colored solid, yield: 205 mg (59.8%); mp: 181-183 °C; ¹H NMR (500 MHz, DMSO-*d*₆); δ 1.85-1.92 (m, 2H, -CH₂), 1.92-2.00 (m, 2H, -CH₂), 2.57 (t, *J* = 5.9 Hz, 2H, -CH₂), 2.89-2.97 (m, 2H, -CH₂), 3.89 (s, 3H, -OCH₃), 3.94 (s, 6H, -OCH₃), 6.71 (s, 1H, ArH), 7.0 (s, 2H, ArH), 7.50 (s, 1H, ArH); IR (KBr) ($\nu_{\max}/\text{cm}^{-1}$): ν = 3144, 3060, 2927, 2854, 1680, 1588, 1503, 1565, 1423, 1312, 1245, 1191, 1036, 1004 cm^{-1} ; MS (ESI) *m/z* 343[M+H]; HR-MS (ESI) *m/z* for C₁₉H₂₃O₄N₂ calculated *m/z*: 343.1653, found *m/z*: 343.1653. Purity (HPLC): 97.15%.

5.5.3. (*E*)-2-((3-(3,4,5-trimethoxyphenyl)-1*H*-pyrazol-5-yl)methylene)-3,4-dihydronaphthalen-1(2*H*)-one (**17c**):

This compound was prepared using the procedure described above by the addition of **12a** (262 mg 1.0 mmol) and 3,4-dihydronaphthalen-1(2*H*)-one (146 mg 1.0 mmol). Yellow colored solid, yield: 245 mg (62.8%); mp: 199-200 °C; ¹H NMR (500 MHz, DMSO-*d*₆); δ 3.08 (t, 2H, *J* = 6.7 Hz -CH₂), 3.30 (t, 2H, *J* = 6.7 Hz, -CH₂), 3.90 (s, 6H, -OCH₃), 3.98 (s, 3H, -OCH₃), 6.79 (s, 1H, ArH), 7.0 (s, 3H, ArH), 7.30 (d, 1H, *J* = 7.5 Hz, ArH), 7.39 (dd, 1H, *J* = 7.5 Hz, ArH), 7.70-7.75 (m, 1H, ArH), 8.13 (d, 1H, *J* = 7.5 Hz, ArH); ¹³C NMR (75 MHz, DMSO-*d*₆); δ 26.5, 56.0, 60.0, 102.8, 126.8, 126.9, 127.2, 128.4, 133.4, 143.5, 153.1, 186.9 ppm; IR (KBr) ($\nu_{\max}/\text{cm}^{-1}$): ν = 3275, 2937, 2837, 1652, 1587, 1517, 1468, 1428, 1313, 1234, 1119, 1030, 1006 cm^{-1} ; MS (ESI) *m/z* 391 [M+H]; HR-MS (ESI) *m/z* for C₂₃H₂₃O₄N₂ calculated *m/z*: 391.1652, found *m/z*: 391.1652. Purity (HPLC): 96.62%.

5.5.4. *(E)*-2-((3-(3,4,5-trimethoxyphenyl)-1*H*-pyrazol-5-yl)methylene)-2,3-dihydro-1*H*-inden-1-one (**17d**):

This compound was prepared using the procedure described above by the addition of **12a** (262 mg 1.0 mmol) and 2,3-dihydro-1*H*-inden-1-one (132 mg 1.0 mmol). The compound obtained as yellow colored solid Yield: 275 mg (73%); mp: 188-190 °C; ¹H NMR (500 MHz, DMSO-d₆); δ 2.60 (s, 2H, -CH₂), 3.88 (s, 3H, -OCH₃), 3.98 (s, 6H, -OCH₃), 6.84 (s, 1H, ArH), 7.08 (dd, 1H, *J* = 10.0 Hz, ArH), 7.47 (s, 4H, ArH), 7.67 (d, 1H, *J* = 10.0 Hz ArH), 7.88 (d, 1H, *J* = 7.9 Hz ArH); IR (KBr) (ν_{max}/cm⁻¹): ν = 3217, 2939, 1682, 1626, 1594, 1504, 1468, 1403, 1331, 1308, 1249, 1126, 1043, 1004 cm⁻¹; MS (ESI) *m/z* 377 [M+H]; HR-MS (ESI) *m/z* for C₂₀H₁₇O₃ N₃Cl calculated *m/z*: 377.1477, found *m/z*: 377.1478. Purity (HPLC): 97.53%.

5.5.5. *(E)*-5-methoxy-2-((3-(3,4,5-trimethoxyphenyl)-1*H*-pyrazol-5-yl)methylene)-2,3-dihydro-1*H*-inden-1-one (**17e**):

This compound was prepared using the procedure described above by the addition of **12a** (262 mg 1.0 mmol) and 5-methoxy-2,3-dihydro-1*H*-inden-1-one (162 mg 1.0 mmol). Yellow colored solid, yield: 280 mg (68.9%); mp: 196-197 °C; ¹H NMR (500 MHz, DMSO-d₆); δ 1.26 (s, 2H, CH₂), 3.86 (s, 3H, -OCH₃), 3.94 (s, 3H, -OCH₃), 3.96 (s, 6H, -OCH₃), 6.80 (s, 1H, ArH), 6.97 (d, 1H, *J* = 8.1 Hz, ArH), 7.06-7.09 (m, 2H, ArH), 7.54 (s, 1H, ArH), 7.60 (s, 1H, ArH), 7.79 (d, 1H, *J* = 8.3 Hz, ArH); ¹³C NMR (75 MHz, DMSO-d₆); δ 27.1, 33.8, 54.2, 58.2, 101.0, 113.4, 123.4, 146.5, 151.3, 163.1, 189.7 ppm; IR (KBr) (ν_{max}/cm⁻¹): ν = 3241, 3120, 2925, 2847, 1686, 1634, 1603, 1517, 1467, 1426, 1444, 1253, 1127, 1023, 1000 cm⁻¹; MS (ESI) *m/z* 407 [M+H]; HR-MS (ESI) *m/z* for C₂₃H₂₃O₅N₂ calculated *m/z*: 407.1609, found *m/z*: 407.1610. Purity (HPLC): 95.91%.

5.5.6. *(E)*-5,6-dimethoxy-2-((3-(3,4,5-trimethoxyphenyl)-1*H*-pyrazol-5-yl)methylene)-2,3-dihydro-1*H*-inden-1-one (**17f**):

This compound was prepared using the procedure described above by the addition of 3-(3,4,5-trimethoxyphenyl)-1*H*-pyrazole-5-carbaldehyde (**12a**) (262 mg 1.0 mmol) and 5,6-dimethoxy-2,3-dihydro-1*H*-inden-1-one (192 mg 0.0659 mmol). Yellow colored solid, yield: 290 mg (66.4%); mp: 184-185 °C; ¹H NMR (500 MHz, DMSO-d₆); δ 2.59 (s, 2H, CH₂), 3.87 (s, 3H, -OCH₃), 3.96 (s, 6H, -OCH₃), 4.01 (s, 6H, -OCH₃), 6.79 (s, 1H, ArH), 7.08 (s, 2H, ArH), 7.317 (s, 1H, ArH), 7.46-7.65 (m, 2H, ArH); ¹³C NMR (75 MHz, DMSO-d₆); δ 30.84, 59.27, 60.34, 103.08, 104.26, 123.78, 126.92, 127.93, 135.30, 137.77, 149.99, 153.45, 193.51 ppm; IR (KBr)

($\nu_{\max}/\text{cm}^{-1}$): $\nu = 3258, 2924, 2850, 1681, 1631, 1589, 1502, 1469, 1428, 1311, 1233, 1129, 1098, 1033, 916 \text{ cm}^{-1}$; MS (ESI) m/z 437 [M+H]; HR-MS (ESI) m/z for $\text{C}_{24}\text{H}_{24}\text{O}_6\text{N}_2$ calculated m/z : 437.1696, found m/z : 437.1696. Purity (HPLC): 96.54%.

5.6. Synthesis of (*E*)-1-substitutedphenyl-3-(3-(3,4,5-trimethoxyphenyl)-1*H*-pyrazol-5-yl)prop-2-en-1-one **18(a-f)**:

To the 3-(benzo[d][1,3]dioxol-5-yl)-1*H*-pyrazole-5-carbaldehyde (**12b**) prepared in the previous step was added corresponding substituted acetophenones and catalytic amount of sodium hydroxide in ethanol. The reaction mixture was stirred at room temperature for 3-4 h and progress of the reaction was monitored by TLC. After completion, ethanol was evaporated under vacuum and the residue was neutralised with dilute HCl solution. Finally the chalcones were extracted with ethyl acetate followed by purification was done by using column chromatography to obtain pure compounds of **18a-f** with good yields (60-75%).

5.6. 1. (*E*)-4-(3-(benzo[d][1,3]dioxol-5-yl)-1*H*-pyrazol-5-yl)but-3-en-2-one (**18a**):

This compound was prepared using the procedure described above by the addition of 3-(benzo[d][1,3]dioxol-5-yl)-1*H*-pyrazole-5-carbaldehyde **12b** (216 mg 1.0 mmol) and propan-2-one (58 mg 1.0 mmol). Yellow colored solid, yield: 191 mg (76%); mp: 201-203 °C; ^1H NMR (500 MHz, DMSO-d_6); δ 2.33 (s, 3H, CH_3), 6.02 (s, 2H, OCH_2O), 6.69 (d, 1H, $J = 16.2 \text{ Hz}$ trans H), 6.82 (s, 1H, Ar H), 6.86 (d, 1H, $J = 7.9 \text{ Hz}$, Ar H), 7.08-7.17 (m, 1H, Ar H), 7.21-7.26 (m, 1H, Ar H), 7.46 (d, 1H, $J = 16.2 \text{ Hz}$ trans H); ^{13}C NMR (75 MHz, DMSO-d_6); δ 27.5, 99.4, 104.0, 106.7, 117.3, 123.8, 125.6, 126.3, 145.5, 146.1, 195.8 ppm; IR (KBr) ($\nu_{\max}/\text{cm}^{-1}$): $\nu = 3220, 2928, 2872, 1764, 1685, 1630, 1581, 1462, 1424, 1353, 1326, 1287, 1045, 960 \text{ cm}^{-1}$; MS (ESI) m/z 257 [M+H]; HR-MS (ESI) m/z for $\text{C}_{14}\text{H}_{13}\text{O}_3\text{N}_2$ calculated m/z : 257.0917, found m/z : 257.0917. Purity (HPLC): 95.70%.

5.6. 2. (*E*)-2-((3-(benzo[d][1,3]dioxol-5-yl)-1*H*-pyrazol-5-yl)methylene)cyclohexanone (**18b**):

This compound was prepared using the procedure described above by the addition of **12b** (216 mg 1.0 mmol) and cyclohexanone (98 mg 1.0 mmol). Pale yellow colored solid, yield: 210 mg (70.9%); mp: 193-195 °C; ^1H NMR (300 MHz, DMSO-d_6); δ 1.76-1.98 (m, 4H, $-\text{CH}_2-$), 2.42-2.61 (m, 2H, $-\text{CH}_2-$), 2.91 (s, 2H, $-\text{CH}_2-$), 6.01 (s, 2H, OCH_2O), 6.64 (s, 1H, Ar H), 6.85 (d, 1H, $J = 7.9 \text{ Hz}$ Ar H), 7.28-7.34 (m, 1H, Ar H), 7.45 (s, 1H Ar H), 7.54 (s, 1H, Ar H); ^{13}C NMR (75 MHz, DMSO-d_6); δ 20.7, 21.0, 26.5, 31.6, 99.2, 101.7, 103.9, 106.5, 117.1, 133.1, 145.2, 145.9, 197.3 ppm; IR (KBr) ($\nu_{\max}/\text{cm}^{-1}$): $\nu = 3197, 3096, 2932, 2883, 1699, 1662, 1578, 1463, 1434,$

1250, 1203, 1153, 969 cm^{-1} ; MS (ESI) m/z 297 [M+H]; HR-MS (ESI) m/z for $\text{C}_{17}\text{H}_{17}\text{O}_3\text{N}_2$ calculated m/z : 297.1232, found m/z : 297.1233. Purity (HPLC): 97.30%.

5.6. 3. (*E*)-2-((3-(benzo[*d*][1,3]dioxol-5-yl)-1*H*-pyrazol-5-yl)methylene)cyclohexanone (**18c**):

This compound was prepared using the procedure described above by the addition of **12b** (216 mg 1.0 mmol) and 3,4-dihydronaphthalen-1(2*H*)-one (146 mg 1.0 mmol). Yellow colored solid Yield: 245 mg (71.2%); mp: 189-190 °C; ^1H NMR (500 MHz, DMSO-d_6); δ 2.58 (s, 2H, $-\text{CH}_2-$), 4.03 (s, 2H, $-\text{CH}_2-$), 6.01 (s, 2H, OCH_2O), 6.77 (s, 1H, $=\text{CH}$), 6.87 (d, 1H, $J = 7.8$ Hz, ArH), 7.28-7.36 (m, 1H, ArH), 7.40-7.50 (m, 3H, ArH), 7.58-7.68 (m, 2H ArH), 7.86 (d, 1H, $J = 7.8$ Hz, ArH); ^{13}C NMR (75 MHz, DMSO-d_6); δ 26.1, 27.1, 100.1, 102.5, 105.1, 107.5, 118.3, 124.3, 125.9, 127.3, 132.2, 133.5, 142.4, 146.7, 146.9, 186.0 ppm; IR (KBr) ($\nu_{\text{max}}/\text{cm}^{-1}$): $\nu = 3229, 3145, 3028, 2882, 1658, 1605, 1584, 1487, 1457, 1411, 1243, 1132, 1037, 977$ cm^{-1} ; MS (ESI) m/z 345 [M+H]; HR-MS (ESI) m/z for $\text{C}_{21}\text{H}_{17}\text{O}_3\text{N}_2$ calculated m/z : 345.1235, found m/z : 345.1235. Purity (HPLC): 96.58%.

5.6.4. (*E*)-2-((3-(benzo[*d*][1,3]dioxol-5-yl)-1*H*-pyrazol-5-yl)methylene)-2,3-dihydro-1*H*-inden-1-one (**18d**):

This compound was prepared using the procedure described above by the addition of **12b** (216 mg 1.0 mmol) and 2,3-dihydro-1*H*-inden-1-one (132 mg 1.0 mmol). Yellow colored solid, yield: 270 mg (81%); mp: 177-178 °C; ^1H NMR (500 MHz, DMSO-d_6); δ 4.05 (s, 2H, $-\text{CH}_2-$), 6.02 (s, 2H, $-\text{OCH}_2\text{O}-$), 6.80 (s, 1H, $=\text{CH}$), 6.88 (d, 1H, $J = 7.7$ Hz, ArH), 7.28-7.38 (m, 1H, ArH), 7.40-7.50 (m, 1H, ArH), 7.56 (s, 2H ArH), 7.60-7.71 (m, 2H, ArH), 7.85 (d, 1H, $J = 7.5$ Hz, ArH); IR (KBr) ($\nu_{\text{max}}/\text{cm}^{-1}$): $\nu = 3238, 2920, 1697, 1636, 1606, 1496, 1463, 1325, 1243, 1201, 1105, 1034$ cm^{-1} ; MS (ESI) m/z 331 [M+H]; HR-MS (ESI) m/z for $\text{C}_{20}\text{H}_{15}\text{O}_3\text{N}_2$ calculated m/z : 331.1085, found m/z : 331.1085. Purity (HPLC): 97.44%.

5.6.5. (*E*)-2-((3-(benzo[*d*][1,3]dioxol-5-yl)-1*H*-pyrazol-5-yl)methylene)-5-methoxy-2,3-dihydro-1*H*-inden-1-one (**18e**):

This compound was prepared using the procedure described above by the addition of **12b** (216 mg 1.0 mmol) and 5-methoxy-2,3-dihydro-1*H*-inden-1-one (162 mg 1.0 mmol). Yellow colored solid, yield: 260 mg (72.2%); mp: 184-186 °C; ^1H NMR (400 MHz, DMSO-d_6); δ 3.94 (s, 3H, $-\text{OCH}_3$), 3.99 (s, 2H, $-\text{CH}_2$), 6.02 (s, 2H, OCH_2O), 6.77 (s, 1H, ArH), 6.85-6.92 (m, 1H, ArH), 6.97 (d, 1H, $J = 7.9$ Hz, ArH), 7.06 (s, 1H, ArH), 7.28-7.36 (m, 1H ArH), 7.54-7.66 (m, 2H, ArH), 7.78 (d, 1H, $J = 8.9$ Hz, ArH); ^{13}C NMR (75 MHz, DMSO-d_6); δ 27.7, 55.1, 101.8, 102.7,

123.6, 126.5, 134.1, 152.3, 199.0 ppm; IR (KBr) ($\nu_{\max}/\text{cm}^{-1}$): $\nu = 3293, 2920, 2851, 1687, 1632, 1598, 1546, 1512, 1464, 1338, 1294, 1140, 1111, 966 \text{ cm}^{-1}$; MS (ESI) m/z 361 [M+H]; HR-MS (ESI) m/z for $\text{C}_{21}\text{H}_{17}\text{O}_4 \text{ N}_2$ calculated m/z : 361.1195, found m/z : 361.1195. Purity (HPLC): 96.78%.

5.6.6. (*E*)-2-((3-(benzo[d][1,3]dioxol-5-yl)-1H-pyrazol-5-yl)methylene)-5,6-dimethoxy-2,3-dihydro-1H-inden-1-one (**18f**):

This compound was prepared using the above procedure by the addition of **12b** (216 mg 1.0 mmol) and 5,6-dimethoxy-2,3-dihydro-1H-inden-1-one (192 mg 0.0659 mmol). Yellow colored solid, yield: 296 mg (76%); mp: 190-192 °C; ^1H NMR (500 MHz, DMSO- d_6): δ 1.24 (s, 2H, -CH₂), 3.93 (s, 3H, -OCH₃), 4.00 (s, 3H, -OCH₃), 6.03 (s, 2H, -OCH₂O-), 6.79 (s, 1H, =CH), 6.84-6.94 (m, 1H, $J = 7.9 \text{ Hz}$ ArH), 7.01-7.18 (m, 1H, ArH), 7.29-7.39 (m, 1H ArH), 7.48-7.51 (m, 1H, ArH), 7.75-7.78 (m, 2H, ArH); ^{13}C NMR (75 MHz, DMSO- d_6): δ 28.0, 55.5, 60.0, 102.2, 103.1, 124.0, 126.9, 134.5, 137.1, 142.5, 148.0, 152.7, 199.4 ppm; IR (KBr) ($\nu_{\max}/\text{cm}^{-1}$): $\nu = 3290, 3136, 2928, 2811, 1680, 1620, 1573, 1480, 1445, 1414, 1362, 1240, 1215, 1155, 1115, 1045, 992 \text{ cm}^{-1}$; MS (ESI) m/z 391 [M+H]; HR-MS (ESI) m/z for $\text{C}_{22}\text{H}_{19}\text{O}_5 \text{ N}_2$ calculated m/z : 391.1285, found m/z : 391.1287. Purity (HPLC): 97.94%.

5.7. Cell culture and reagents: All the cell lines used in this study were obtained from the American Type Culture Collection (ATCC). MCF-7 and MDA-MB-231 (human breast carcinoma cell lines) were grown in Dulbecco's modified Eagle's medium (DMEM) containing non essential amino acids and 10% FBS. All the cells maintained under humidified atmosphere of 5% CO₂ at 37 °C. Cells were trypsinized when sub confluent from T75 flasks/90mm dishes and seeded on to 96 well test plates at a concentration of 1×10^4 cells/mL in complete medium, treated with compounds at desired concentrations and harvested as required.

5.8. Analysis of antiproliferative activity: Cell proliferation and viability was determined by 3-[4,5-dimethylthiazol-2-yl]-2,5-diphenyltetrazolium bromide (MTT) assay. The pale yellow colored tetrazolium salt (MTT) reduces to a dark blue water-insoluble formazan by metabolically active cells and that is measured quantitatively after soluble in DMSO. The absorbance of the soluble formazan is directly proportional to the number of viable cells. Cells were seeded at a density of 1×10^4 cells in 200 μL of medium per well of 96-well plate. The 96-well microtiter plates were incubated for 24 h prior to addition of the experimental compounds. Cells were treated with vehicle alone (0.4% DMSO) or compounds (drugs were dissolved in DMSO

previously) at different concentrations (1, 10 and 25 μ M) of test compounds for 48 hours. The assay was completed with the addition of MTT (5 %, 10 μ L) and incubated for 60 min at 37⁰C. The supernatant was aspirated and plates were air dried and the MTT-formazon crystals dissolved in 100 μ L of DMSO. The optical density (O.D) was measured at 560 nm using TECAN multimode reader. The growth percentage of each treated well of 96 well plate have been calculated based on test wells relative to control wells. The cell growth inhibition was calculated by generating dose response curves as a plot of the percentage of surviving cells versus drug concentration. Antiproliferative activity of the cancer cells to the test compounds was expressed in terms of IC₅₀ value, which defines as a concentration of compound that produced 50% absorbance reduction relative to control.

5.9. Cell cycle distribution analysis: MCF-7 Cells (NCI, USA) were grown to 70% confluency in RPMI medium containing 10% serum at 37⁰C with 5% CO₂ in humidified incubator. Cells were then washed with 1X PBS and incubated in medium containing 0.05% fetal bovine serum (FBS, Invitrogen, USA) for 24 hours for cell cycle synchronization. Later, culture media was replenished with 10% FBS and cells were further incubated for 24 hours in media alone or in presence of conjugates **13c**, **13d**, **16b**, **14d** , **CA-4** at 2 μ M concentration and/ or adriamycin at 1 μ M concentration. After incubation, cells were washed once with 1X PBS and fixed with 70% cold ethanol (S.D. Fine Chemicals, Mumbai) overnight at 4⁰C. Fixed cells were washed with 1X PBS and incubated with RNase A (40 μ g/ml) and Propidium Iodide (40 μ g/ml) for 1hour at 37⁰C. Cells were passed through 26gauge needle 2-3 times to get rid of aggregates. These cells were acquired on FACS Calibre (BD Biosciences, San Vose, USA) and analyzed by ModFit LT 4.1 Verity Software House, Country.

5.8. Detection of mitochondrial membrane potential by DiOC6 staining: MCF-7 cells were cultured in complete medium in a 6- well tray at density of 0.3x10⁶ cells /ml/ well at 37 °C in humidified air with 5% CO₂. Cells were treated with compounds **13c**, **13d**, **16b**, **14d** and **CA-4** at 2 μ M concentration for 18 hours. In another set, cells were CA-4 and 14d at 5 hours separately. After treatment, cells were harvested. For positive control for mitochondrial membrane destabilization 1x10⁶ cells were suspended in 4% freshly prepared paraformaldehyde (Sigma-Aldrich, MO, USA) and incubated at room temperature for 10 min and then washed with prewarmed 1ml PBS three times. DiOC6 ((Life Technologies, Molecular Probes[®] ,USA) dye was added to a concentration of 0.1 μ M to the 1x10⁶ cells per ml. Cells were incubated at 37⁰C for 15

min and washed three times by centrifugation at 1000 rpm for 5 min. Cells were resuspended in 500 μ l PBS and acquired on FACSCalibre (BD Biosciences, USA). Data was analyzed on CellQuest Software (BD Biosciences, USA). Data was represented as histogram overlay, percent cells with depolarized mitochondrial membrane, and mean fluorescence intensity change observed before and after treatment with compounds.

5.9. Detection of apoptosis by Annexin V-FITC and propidium iodide staining: MCF-7 cells were cultured in presence and absence of compounds for 24 hours and then resuspended in 1X Annexin Binding Buffer at a density of 1×10^6 cells per ml. 100 μ l of this suspension was transferred to flow cytometry tubes and mixed with 5 μ l of Annexin V FITC (BD Biosciences, USA) and 1 μ l of Propidium Iodide (40 μ g/ml; Sigma-Aldrich, USA). Cells were gently vortexed and incubated for 15 min at RT in the dark. After incubation 400 μ l of 1X Annexin Binding Buffer was added to each tube and samples were acquired on FACSCalibre (BD Biosciences, USA). Data was analyzed on FlowJo Software (www.flowjo.com). For compensation MCF-7 cells treated with etoposide 50 μ M for 24 hours stained with only PI or only annexin and stained dually with annexin/PI were used.

5.10. Immunofluorescence: MCF-7 cells were seeded on glass cover slips, incubated for 24 h in the presence or absence of test compounds at a final concentration of 2 μ M. Cells grown on cover slips were fixed in 4% formaldehyde in phosphate-buffered saline (PBS) pH 7.4 for 20 min at room temperature. Cells were permeabilized for 5 min in PBS containing 0.5% Triton X-100 (Sigma) and 0.05% Tween-20 (Sigma). The permeabilized cells were blocked with 1% BSA (Sigma) in PBS for 1 h. Later, the cells were incubated with primary antibody diluted in blocking solution for 4 h at room temperature. Subsequently the antibodies were removed and the cells were washed thrice with PBST. Cells were then incubated with secondary antibody for 1 h at room temperature. Cells were washed thrice with PBST and mounted in medium containing DAPI (vecta shield). Images were captured using the Olympus confocal microscope FLOW VIEW FV 1000 series and analyzed with FV10ASW 1.7 series software.

5.11. Western blot analysis: Cells were lysed and lysate was extracted using RIPA lysis buffer after treatment with compounds for 48h at 1 μ M final drug concentration. Protein was quantitated using the Bradford assay and 20 μ g of total protein was loaded per well, and resolved on 8.0%, 10.0%, or 12% SDS-polyacrylamide gels. The gels were then transferred to Immobilon-P, PVDF (Millipore, Billerica, Massachusetts) using semidry transfer technique and probed with the

primary and secondary antibodies. ECL (GE, Pittsburgh, Pennsylvania) was used as the chemiluminescent substrate.⁴⁶⁻⁴⁷

5.11. Real Time PCR(qRT-PCR)

Total RNA was isolated using TRIzol method. cDNA was prepared from the total RNA and Total RNA was isolated using trizol reagent (Invitrogen, USA) from cells treated with compounds for 48h at 1uM final drug concentration and concentrations were quantified at 260nm by NanoDrop 1000 Spectrophotometer (Thermo Fischer scientific, USA). cDna synthesis was done by using RNA to cDNA EcoDry™ Premix (#639543, Clontech Laboratories, Inc., USA). mRNA levels were determined using qRT-PCR. SYBR green (Takara clontech) master mix was used for qRT-PCR analysis by 7900HT Fast Real Time-PCR (Applied Biosystems, USA) using appropriate primers. Reaction mixture of about 10 µl was prepared (2µl of H2O, 1µl of reverse primer, 1µl of forward primer, 5µl of SYBR green premix and 1 ul of Cdna as template). Quantification was done followed by amplification protocol- HotStart (50°C for 2 min), initial denaturation (95 °C for 10 min), denaturation (95°C for 15 sec) annealing and extension (60°C for 1 min) for 40 cycles with each step under fluorescence measurement mode. Standard curves were obtained from amplicons. $\Delta\Delta CT$ method was used to analyze the qRT-PCR data. ACTIN was used for normalization. Primer sequences used were PI3K F-TCTTCTGCAAAAAGGCCACT, R-GAATTTTCGCACCACCTCAAT; Akt F-GCACCTTCCATGTGGAGACT, R-CCCAGCAGCTTCAGGTACTC; PTEN F-ACCAGGACCAGAGGAAACCT, R-GCTAGCCTCTGGATTTGACG; Bcl-2 F-GAGGATTGTGGCCTTCTTTG, R-ACAGTTCCACAAAGGCATCC; BAX F-TTTGCTTCAGGGTTTCATCC, R-CAGTTGAAGTTGCCGTCAGA; p53 F-GTTCCGAGAGCTGAATGAGG, R-TCTGAGTCAGGCCCTTCTGT; and GAPDH F-GAGTCAACGGATTTGGTCGT, R- TTGATTTTGGAGGGATCTCG.

5.12. Molecular Modelling:

AutoDock was used to perform the molecular modelling studies of pyrazolochalcone conjugates at ATP binding site of PI3K γ . Initial Cartesian coordinates for the protein-ligand complex structure were derived from crystal structure of PI3K γ (PDB ID: 1E7V).⁴⁸ The protein targets were prepared for molecular docking simulation by removing water molecules, bound ligands. Hydrogen atoms and Kollman charges were added to each protein atom. Auto-Dock Tools (ADT) was used to prepare and analyze the docking simulations for the AutoDock

program. Coordinates of each compound were generated using Chemdraw11 followed by MM2 energy minimization. Grid map in Autodock that defines the interaction of protein and ligands in binding pocket was defined. The grid map was used with 60 points equally in each x, y, and z direction. AutoGrid 4 was used to produce grid maps for AutoDock calculations where the search space size utilized grid points of 0.375 Å. The Lamarckian genetic algorithm was chosen to search for the best conformers. Each docking experiment was performed 100 times, yielding 100 docked conformations. Parameters used for the docking were as follows: population size of 150; random starting position and conformation; maximal mutation of 2 Å in translation and 50 degrees in rotations; elitism of 1; mutation rate of 0.02 and crossover rate of 0.8; and local search rate of 0.06. Simulations were performed with a maximum of 1.5 million energy evaluations and a maximum of 50000 generations. Final docked conformations were clustered using a tolerance of 1.0 Å root mean square deviation. The best model was picked based on the best stabilization energy. Final figures for molecular modeling were generated by using PyMol.⁴⁹⁻⁵⁰

Associated content

Supporting Information

¹H NMR and ¹³C NMR spectra of final compounds and five dose results of selected compounds and HPLC spectra for biologically best active compounds have been provided.

Author information

Conception and design: A. Kamal (Chemistry study), A. Juvekar, J. Kode, M.P. Bhadra (Biological study)

Development of methodology, acquisition of data, analysis and interpretation of data: A. Kamal, A. B. Shaik (Chemistry study), G. K. Rao, G. B. Kumar, N. Patel, V. S. Reddy, I. Khan, M. Barkume, S. Jadhav, A. Juvekar, J. Kode, M.P. Bhadra (Biological study).

Writing, review, and/or revision of the manuscript: A. Kamal, M.P. Bhadra, A. B. Shaik, (IICT), J. Kode (ACTREC).

Financial support: A. Kamal (IICT), A. Juvekar, J. Kode (ACTREC)

Corresponding author Tel.: +91-40-27193157; fax: +91-40-27193189, e-mail: ahmedkamal@iiict.res.in (A. Kamal).

Notes

The authors declare no competing financial interest.

Acknowledgments

A.B.S, G.B.K and S.J. would like to acknowledge CSIR, New Delhi and G.K. would like to thank the University Grant Commission, New Delhi for the award of senior research fellowships. Authors would like to thank Council of Scientific and Industrial Research, Government of India for financial support under the 12th Five Year plan project “Affordable Cancer Therapeutics” (CSC0301) and “Small Molecules in Lead Exploration (SMiLE)” (CSC0111).

References

- [1] D. A. Fruman, R. E. Meyers, L. C. Cantley. *Annu. Rev. Biochem.* 67 (1998) 481–507.
- [2] B. T. Hennessy, D. L. Smith, P. T. Ram, Y. Lu, G. B. Mills. *Nat. Rev. Drug Discov.* 4 (2005) 988–1004.
- [3] Y. L. Chen, P. Y. Law, H. H. Loh. *Curr. Med. Chem. Anticancer Agents.* 5 (2005) 575–589.
- [4] M. P. Wymann, M. Zvelebil, M. Laffargue. *Trends Pharmacol. Sci.* 24 (2003) 366–376.
- [5] J. Yuan, P. P. Mehta, M. J. Yin, S. Sun, A. Zou, J. Chen, K. Rafidi, Z. Feng, J. Nickel, J. Engebretsen, J. Hallin, A. Blasina, E. Zhang, L. Nguyen, M. Sun, P. K. Vogt, A. McHarg, H. Cheng, J. G. Christensen, J. L. Kan, S. Bagrodia. *Mol. Cancer Ther.* 10 (2011) 2189–99.
- [6] S. I. Gharbi, M. J. Zvelebil, S. J. Shuttleworth, T. Hancox, N. Saghir, J. F. Timms, M. D. Waterfield. *Biochem. J.* 404 (2007) 15–21.
- [7] G. J. Brunn, J. Williams, C. Sabers, G. Wiederrecht, Jr. J. C. Lawrence, R. T. Abraham, *EMBO J.* 15 (1996) 5256–5267.
- [8] A. Dittmann, T. Werner, CW. Chung, MM. Savitski, M. Fälth Savitski, P. Grandi, C. Hopf, M. Lindon, G. Neubauer, RK. Prinjha, M. Bantscheff, G. Drewes. *ACS Chem Biol.* 9(2) (2014) 495–502.
- [9] A. Murakami, H. Ashida, J. Terao. *Cancer Lett.* 269 (2008) 315–325.
- [10] X. L. Tan, S. D. Spivack, *Lung Cancer.* 65 (2009) 129–137.
- [11] T. Hirano, K. Abe, M. Gotoh, K. Oka. *Br. J. Cancer.* 72 (1995) 1380–1388.
- [12] M. Liu, H. Yin, X. Qian, J. Dong, Z. Qian, J. Miao. *Molecules.* 22(1) (2016) pii: E36.
- [13] M. E. Prime, S. M. Courtney, F. A. Brookfield, R. W. Marston, V. Walker, J. Warne, A. E. Boyd, N. A. Kairies, W. von der Saal, A. Limberg, G. Georges, R. A. Engh, B. Goller, P. Ruege, M. Rueth. *J. Med. Chem.* 54 (2011) 312–319.

- [14] H. Minegishi, Y. Futamura, S. Fukashiro, M. Muroi, M. Kawatani, H. Osada, H. Nakamura, *J. Med. Chem.* 58 (2015) 4230-4241.
- [15] A. Kamal, A. B. Shaik, S. Polepalli, V. S. Reddy, G. B. Kumar, S. Gupta, K. V. Krishna, A. Nagabhushana, R. K. Mishra, N. Jain. *Org. Biomol. Chem.* 12 (2014) 7993-8007.
- [16] B. Abu Thaher, M. Arnsmann, F. Totzke, J. E. Ehlert, M. H. Kubbutat, C. Schächtele, M. O. Zimmermann, P. Koch, F. M. Boeckler, S. A. Laufer. *J. Med. Chem.* 55 (2012) 961-965.
- [17] C. Zhuang, Z. Miao, Y. Wu, Z. Guo, J. Li, J. Yao, C. Xing, C. Sheng, W. Zhang. *J. Med. Chem.* 57 (2014) 567-577.
- [18] S. M. Kim, S. W. Lee, Y. H. Song. *Bull. Korean Chem. Soc.* 35 (2014) 2859-2862.
- [19] E. Therrien, G. Larouche, N. Nguyen, J. Rahil, A. M. Lemieux, Z. Li, M. Fournel, T. P. Yan, A. J. Landry, S. Lefebvre, J. J. Wang, K. MacBeth, C. Heise, A. Nguyen, J. M. Besterman, R. Déziel, A. Wahhab. *Bioorg. Med. Chem. Lett.* 25 (2015) 2514-2518.
- [20] G. B. Park, D. Y. Hur, D. Kim. *Anticancer Res.* 35 (2015) 2699-708.
- [21] R. Jorda, L. Havlíček, I. W. McNae, M. D. Walkinshaw, J. Voller, A. Sturc, J. Navrátilová, M. Kuzma, M. Mistrík, J. Bártek, M. Strnad, V. Krystof. *J. Med. Chem.* (2011) 54 2980-2993.
- [22] E. Buchner, M. Fritsch. *Liebigs Ann.* (1893) 273 256-266.
- [23] H. T. Foley, B. I. Schnider, G. L. Gold, Y. Uzer. *Cancer Chemother. Rep.* (1965) 44 45-48.
- [24] E. B. Yang, Y. J. Guo, K. Zang, Y. Z. Chen, P. Mack. *Biochim. Biophys. Acta.* (2001) 11, 144-152.
- [25] YN. Liu, JJ. Wang, YT. Ji, GD. Zhao, LQ. Tang, CM. Zhang, XL. Guo, ZP. Liu. *J Med Chem.* 59(11) (2016) 5341-55.
- [26] H. Ebiike, N. Taka, M. Matsushita, M. Ohmori, K. Takami, I. Hyohdoh, M. Kohchi, T. Hayase, H. Nishii, K. Morikami, Y. Nakanishi, N. Akiyama, H. Shindoh, N. Ishii, T. Isobe, H. Matsuoka. *J Med Chem.* 59(23) (2016) 10586-10600
- [27] S. Yamamoto, E. Aizu, H. Jiang, T. Nakadate, I. Kiyoto, J. C. Wang, R. Kato. *Carcinogenesis.* 12 (1991) 317-323.
- [28] G. Achanta, A. Modzelewska, L. Feng, S. R. Khan, P. Huang. *Mol. Pharmacol.* 70 (2006) 426-433.
- [29] J. Lim, S. H. Lee, S. Cho, I. S. Lee, B. Y. Kang, H. J. Choi. *Mol. Cells.* 36 (2013) 340-346.

- [30] S. Ducki, D. Rennison, M. Woo, A. Kendall, JF. Chabert, AT. McGown, NJ. Lawrence, *Bioorg. Med. Chem.* 17 (2009) 7698-710.
- [31] P. Wu, YZ. Hu, *Curr Med Chem.* 17 (35) (2010) 4326-4341.
- [32] HL. Ng, X. Ma, EH. Chew, WK. Chui, *J Med Chem.* (2017) doi:10.1021/acs.jmedchem.6b01253.
- [33] SA. Ejaz, A. Saeed, MN. Siddique, ZU. Nisa, S. Khan, J. Lecka, J. Sévigny, J. Iqbal, *Bioorg Chem.* pii: S0045-2068 (16) (2017) 30349-30352.
- [34] J. Wei, H. Zhu, G. Lord, M. Bhattachayya, BM. Jones, G. Allaway, SS. Biswal, B. Korman, RG. Marangoni, WG. Tourtellotte, J. Varga, *Transl Res.* pii: S1931-5244 (16) (2016) 30422-30424.
- [35] J. Jr. Polivka, F. Janku. *Pharmacol Ther.* 142 (2) (2014) 164-175.
- [36] R. Dienstmann, J. Rodon, V. Serra, J. Tabernero. *Mol Cancer Ther.* 13 (5) (2014) 1021-1031.
- [37] P. Xia, X. Y. Xu, *Am. J. Cancer Res.* 5 (2015) 1602-1609.
- [38] ER. Sharlow, S. Leimgruber, A. Lira, MJ. McConnell, A. Norambuena, GS. Bloom, MW. Epperly, JS. Greenberger, JS. Lazo. *ACS Chem Biol.* 11 (5) (2016) 1428-1437.
- [39] AW. Brown, M. Fisher, GM. Tozer, C. Kanthou, JP. Harrity. *J Med Chem.* 59 (20) (2016) 9473-9488.
- [40] HA. Elshemy, MA. Zaki, *Bioorg Med Chem.* 25(3) (2017) 1066-1075.
- [41] A. Kamal, A. B. Shaik, G. B. Kumar, V. S. Reddy, C. G. Kumar, *International Patent.*, (2015) WO2015029051 A1.
- [42] S. Sidique, R. Ardecky, Y. Su, S. Narisawa, B. Brown, J. L. Millan, E. Sergienko, N. D. Cosford. *Bioorg. Med. Chem. Lett.* 19 (2009) 222-225.
- [43] a) A. Kamal, AB. Shaik, S. Polepalli, GB. Kumar, VS. Reddy, R. Mahesh, S. Garimella, N. Jain, *Bioorg Med Chem.* 23 (2015) 1082-1095. b) A. Kamal, AB. Shaik, GB. Kumar, VS. Reddy, PYRAZOLE LINKED BENZIMIDAZOLE CONJUGATES AND A PROCESS FOR PREPARATION THEREOF. *US Patent.* (2015) 20,150,329,527.
- [44] E. H. Walker, O. Perisic, C. Ried, L. Stephens, R. L. Williams. *Nature.* 402 (1999) 313-320.

- [45] A. Kamal, AB. Shaik, N. Jain, C. Kishor, A. Nagabhushana, B. Supriya, G. BharathKumar, SS. Chourasiya, Y. Suresh, RK. Mishra, A. Addlagatta. *Eur J Med Chem.* 92 (2015) 501-513.
- [46] P. Padmaja, G. Koteswara Rao, A. Indrasena, BV. Subba Reddy, N. Patel, AB. Shaik, N. Reddy, PK. Dubey, MP. Bhadra. *Org Biomol Chem.* 13(5) (2015) 1404-1414.
- [47] JR. Vangala, S. Dudem, N. Jain, SV. Kalivendi. *J Biol Chem.* 289(18) (2014) 12612-1222.
- [48] E. H. Walker, M. E. Pacold, O. Perisic, L. Stephens, P. T. Hawkins, M. P. Wymann, R. L. Williams *Mol. Cells.* 6 (2000) 909-919.
- [49] AutoDock, version 4.0; <http://www.scripps.edu/mb/olson/doc/autodock/>.
- [50] W. L. DeLano, DeLano Scientific, San Carlos, CA, USA, <http://www.pymol.org.>, (2002).

Figure Captions

Figure 1. Chemical structures of some potential anticancer agents: PF-4691502 (**1**), Wortmannin (**2**), LY294002 (**3a**), Quercetin (**3b**), Tangeretin (**3c**), Doxorubicin (**4**), Pyrazole restricted CA-4 (**5a**), Dihydropyridopyrazoles (**5b**), Pyridinyl pyrazole (**5c**), Flavokawain B (**6**), SD400 (**7**). SAR of pyrazolechalcone conjugates (**8**).

Figure 2. Panel A gives percent DiOC6+ cells which were gated for M2 region (**C-b**) and categorized as those with depolarized mitochondria. **Panel B** exhibits mean fluorescence intensity of MCF-7 cells gated in region M1 categorized as MCF-7 control region. **Panel C** shows overlay of histograms of MCF-7 treated with conjugates positive control (PFA, **(c)**), CA-4 (**(d)**), **13c (e)**, **13d (f)**, **16b (g)** and **14d (h)**. **(a)** gives dot plot of MCF-7 cells used, while **(b)** shows gating strategy for MCF-7 control DiOC6 labelled cells (M2 region) and cells with depolarized mitochondria (M1 region). Note: **13c (TCH6)**, **13d (TCH12)**, **16b (TCH36)** and **14d (TCH39)**. (Experiment was repeated two times and representative data is provided).

Figure 3. Shows cell cycle stages of MCF-cells treated with conjugates for 24 hours (A, B) and 48 hours (C, D). B and D provide overlay cell cycle phases of conjugates in comparison to MCF-7 in medium alone. Conjugates **CA-4 (c)**, **13c (e)**, **13d (f)**, **16b (g)** and **14d (h)** were tested at 2 μ M concentration while ADR was used at 2 μ M concentration (**d**) to treat MCF-7 cells. Lymphocyte control served as diploid control (2n chromosomes; **a**) and MCF-7 cells in medium

alone swerved as cell control (**b**). (Experiment was repeated two times and representative data is provided).

Figure 4. Panel 1. Apoptosis detection in MCF-7 cells. MCF-7 cells were treated with conjugates at 2 μ M concentration or in medium alone for 48 h and stained by Annexin FITC/PI. **Panel A** gives percent early apoptotic, late apoptotic and necrotic population in MCF-7 cells untreated and treated with **CA-4** and conjugates **13c**, **13d**, **16b** and **14d**. **Panel B** gives dot plot of stained cells compensated using MCF-7 treated with only PI and MCF-7 treated with only annexin-FITC. Dot plot represent MCF-7 cells untreated (panel a) and treated with **CA-4** (**b**) and conjugates **13c** (**c**), **13d** (**d**), **16b** (**e**) and **14d** (**f**). The figures on top right of each panel gives percent positive cells in four quadrants as lower right (early apoptotic), upper right (late apoptotic and upper left (necrotic). (Experiment was repeated two times and representative data is provided).

Figure 5. Effect on PI3K/Akt/mTOR pathway. (A) MCF-7 cells were seeded on cover glass and treated with **13b**, **13c**, **13d**, **16b** and **14d** at 2 μ M concentration for 48 h followed by Immunofluorescence assay. RED color in the panel indicates the Akt protein and BLUE indicates DAPI nuclear DNA staining. Merge indicates both DAPI (BLUE) and Akt (RED). UT is untreated and LY294002 is the positive control. (B) Protein lysate was collected from the treated cells and a panel of proteins was analyzed using Western blotting technique. The Beta actin served as gel loading control. (C) mRNA was collected from the treated cells and subjected to qRT-PCR after cDNA conversion for relative mRNA expression changes of respective genes, Error bars indicate the Standard Deviation. (Experiment was repeated three times and representative data is provided).

Figure 6. A. Docking pose illustrates the binding simulations of **13c** (green sticks) at phosphatidylinositol 3-kinase catalytic subunit. Blue stick represents interaction of selected amino acid via significant hydrogen bonds, while the blue lines indicate the amino acid residues that exhibit hydrophobic interactions. The hydrogen bonds are shown by red dotted lines. B. Indicates the superimposition of **13c** at the catalytic site of PI3K γ . The green sticks represent the inhibitors (**13c** and **LY294002**), whereas the yellow and orange sticks indicate the group of amino acid residues at the catalytic site (mesh). The last pose indicates the superimposition of **13c** on **LY294002** at the catalytic site of PI3K γ . The inhibitors **13c** and **LY294002** are shown in green and yellow sticks, respectively.

Figure 7. Images representing docking poses of **13c**, **13d**, **14d** and **16b** (green sticks) at phosphatidylinositol 3-kinase (PI3K) catalytic subunit (light orange cartoon). Blue stick represents selected amino acids with interactions via hydrogen bonding, while blue and light orange lines indicate hydrophobic interactions. Red dotted lines illustrate hydrogen bonds. All the active ligands exclusively form a significant hydrogen bonding interactions with well recognized amino acid residue Val-882. Images were visualized by PyMoL.

Table 1. *In vitro* cytotoxicity of pyrazolochalcones **13 (b-e, h-j)**, **14 (c,d)**, **15 (a, c-d)**, **16 (b, d)**, and **18f** in a panel of sixty cancer cell lines.

Table 2. Structures of pyrazolochalcone conjugates (**13-14a-j**, **15-16a-d** and **17-18a-e**) and cytotoxic activity against MCF-7 and MDA-MB-231 ($IC_{50} \pm SD$).

Scheme 1. Synthesis of pyrazolochalcones: *Reagents and conditions*; (i) Diethyl oxalate/NaOEt/ethanol, 4h, 0 °C-rt, (80-90%); (ii) $NH_2-NH_2 \cdot 2HCl$ /ethanol, 3 h, reflux, (70-75%); (iii) $LiAlH_4$ /THF, 2 h, 0 °C-rt, (70-80%); (iv) IBX/dry DMSO, 1h, rt, (80-90%); (v) NaOH/ ethanol, different acetophenones/indanones, 3-4 h, rt, (60-75%).

Scheme 2. Synthesis of pyrazolochalcones (**17a-f**): *Reagents and conditions*: (i) NaOH/EtOH, different ketones, 1-2 h, rt (65-75%).

Scheme 3. Synthesis of pyrazolochalcones (**18a-f**): *Reagents and conditions*: (i) NaOH/EtOH, different ketones, 1-2 h, rt (65-75%).

Figure 2

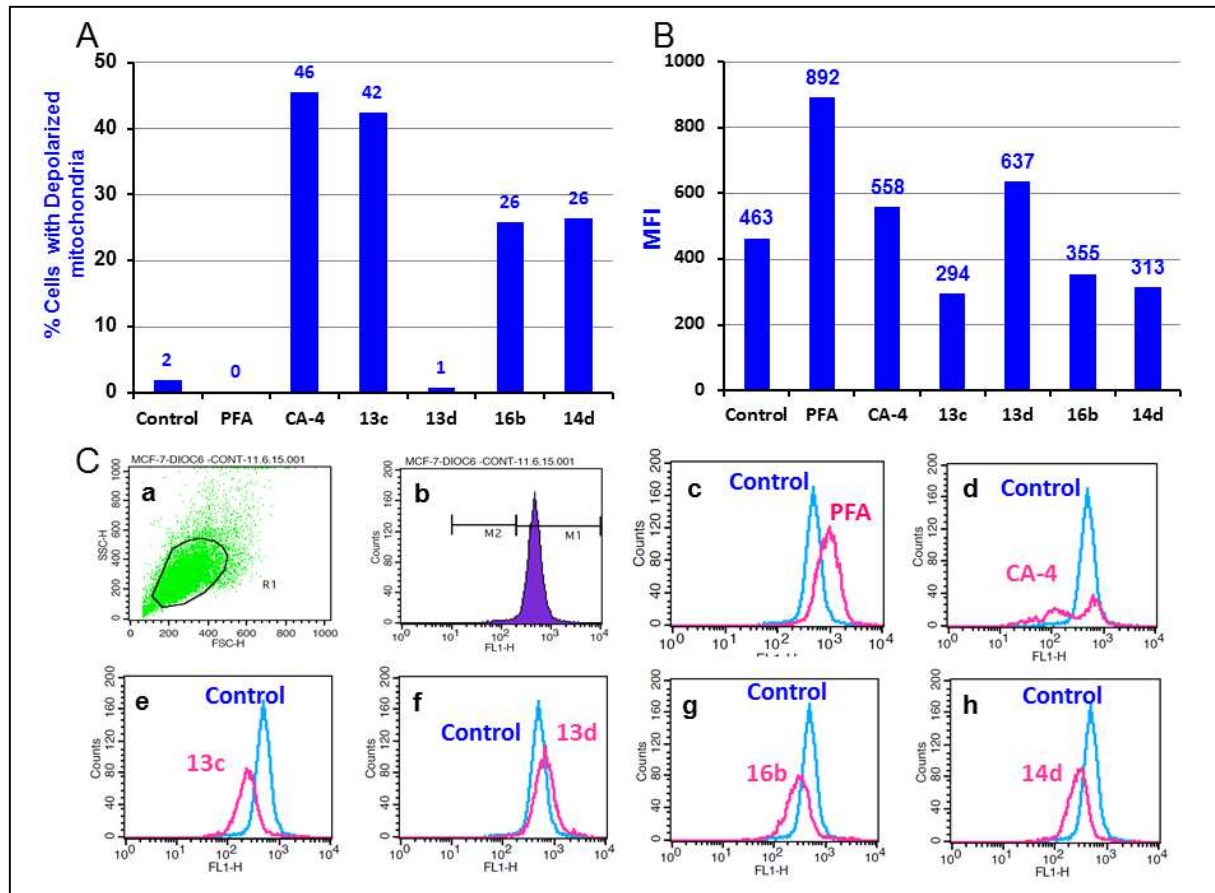


Figure 3

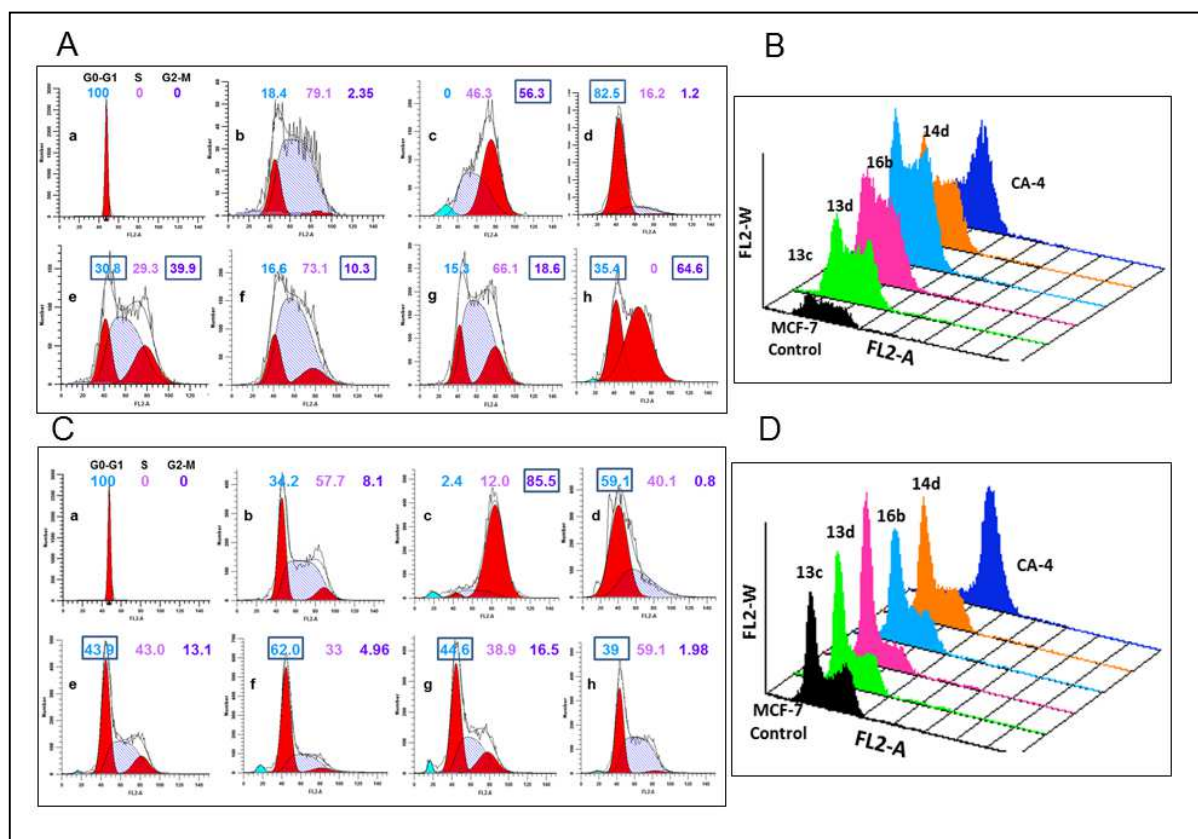


Figure 4

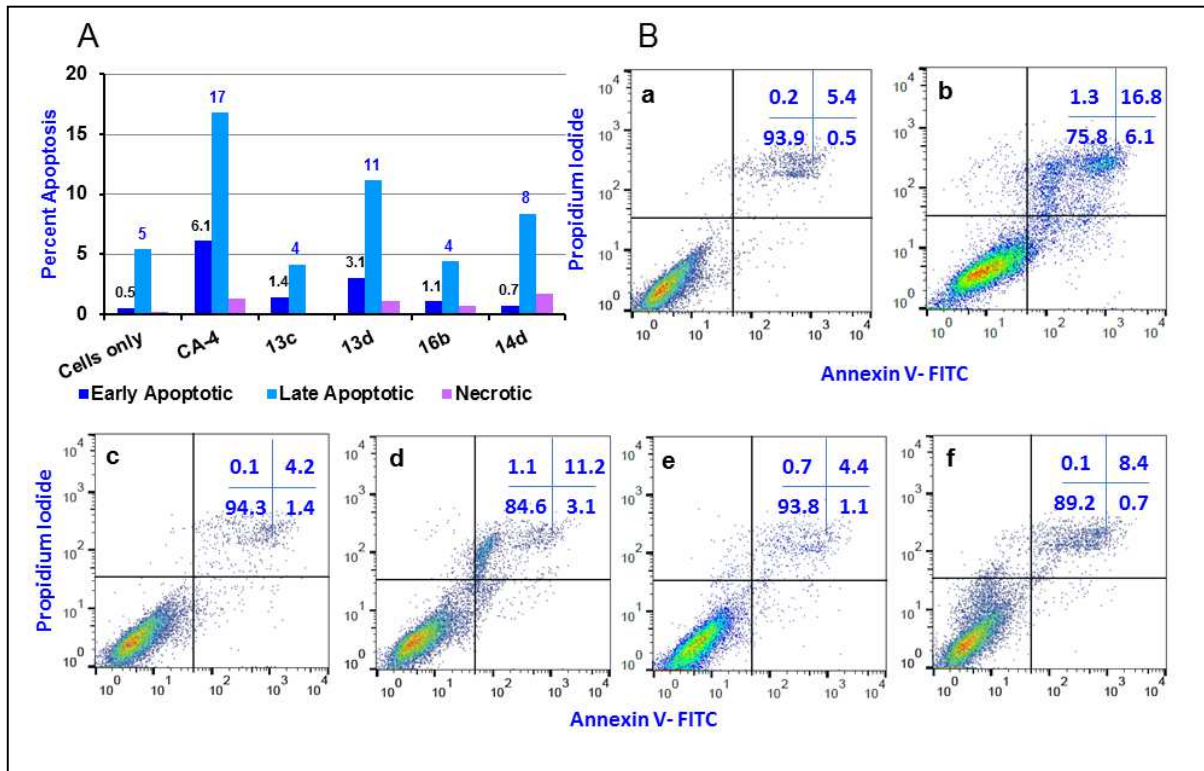


Figure 5

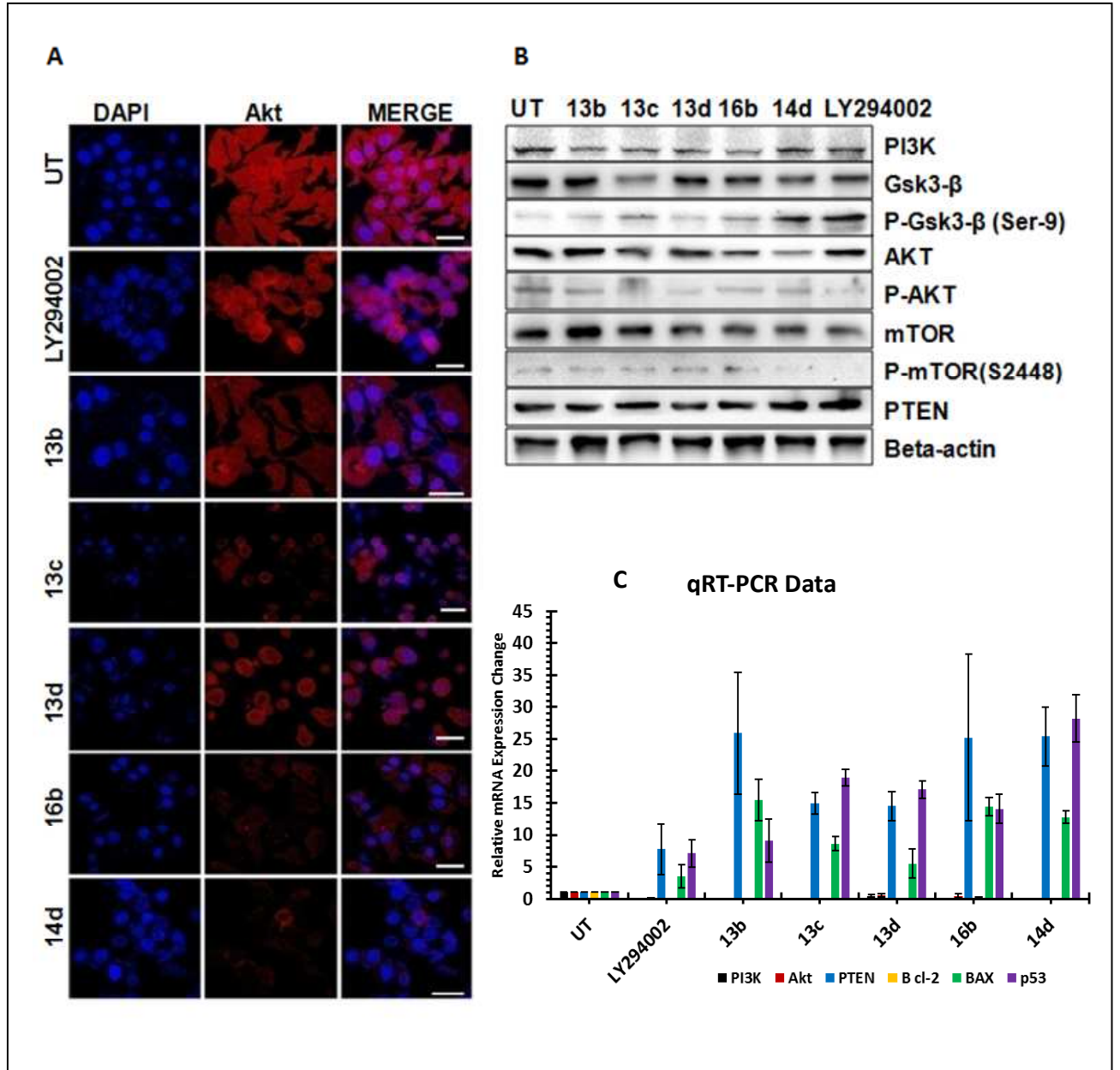
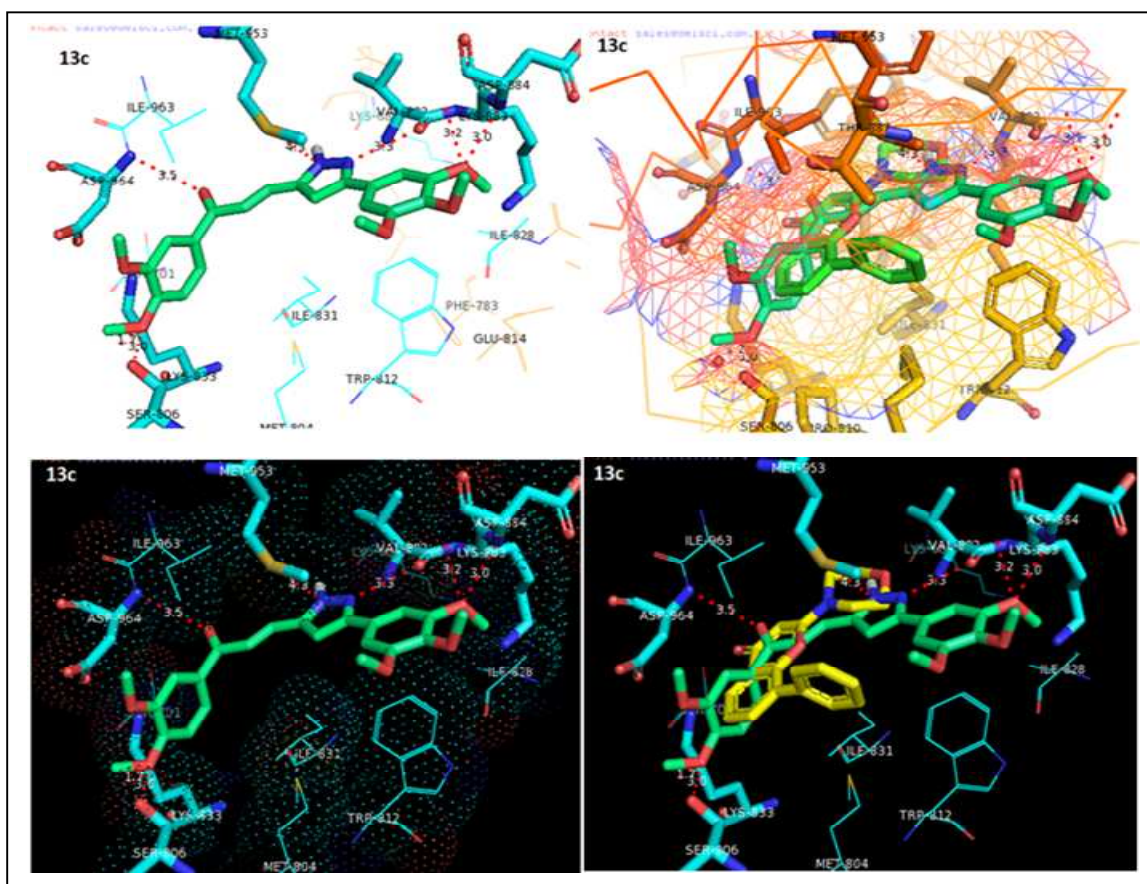


Figure 6



ACCEPTED

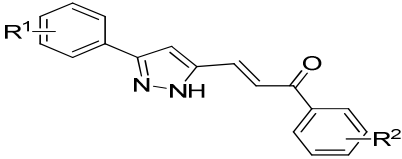
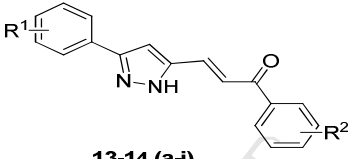
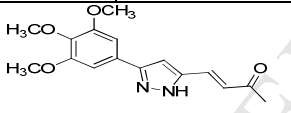
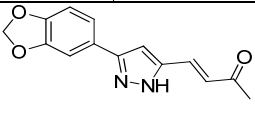
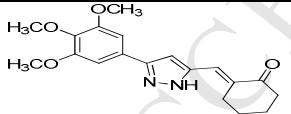
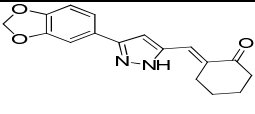
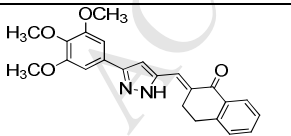
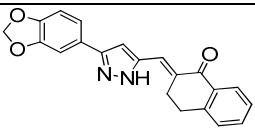
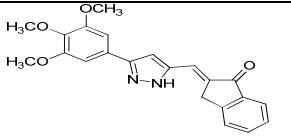
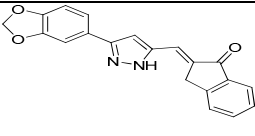
Table 1

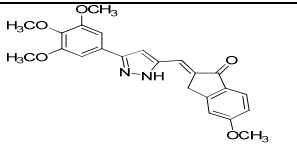
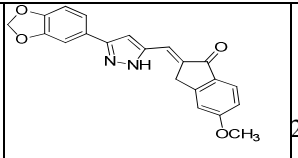
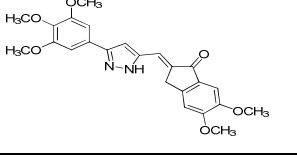
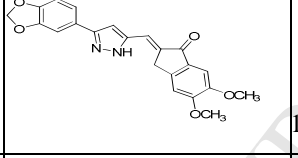
Cancer panel/cell line	^a GI ₅₀ (μM)														
	^b 13b	^c 13c	^d 13d	^e 13e	^f 13h	^g 13i	^h 13j	ⁱ 14c	^j 14d	^k 15a	^l 15c	^m 15d	ⁿ 16b	^o 16d	^p 18f
<i>Leukemia</i>															
CCRF-CEM	1.42	0.62	1.68	1.57	2.15	3.80	0.55	2.52	2.00	0.34	0.36	1.74	1.34	1.32	1.14
HL-60(TB)	2.16	1.44	1.93	2.17	7.18	2.48	1.74	2.82	2.17	1.69	2.76	3.45	2.18	1.43	2.07
K-562	2.32	1.91	2.96	3.20	4.96	3.31	0.72	2.47	2.17	0.73	0.61	2.03	1.28	1.42	1.59
MOLT-4	2.67	2.11	2.32	2.98	4.38	2.72	1.91	3.00	2.71	1.81	2.20	3.11	2.67	2.32	2.57
RPMI-8226	0.43	0.24	0.31	0.51	0.53	1.76	0.47	1.03	0.56	0.29	0.37	1.28	0.32	0.60	0.23
SR	0.34	0.27	0.39	0.55	0.39	2.92	0.32	1.27	1.20	0.20	0.25	0.58	0.67	0.79	0.62
<i>Non-small cell lung</i>															
A549/ATCC	2.27	1.86	2.72	4.32	18.7	2.43	2.08	2.70	2.13	2.39	2.25	2.75	1.88	2.55	1.96
HOP-62	1.76	1.44	1.46	2.18	1.72	4.39	1.77	2.08	2.33	1.45	1.73	2.80	2.35	2.80	1.53
HOP92	1.06	^q	0.86	^q	2.53	^q	3.68	2.16	^q	1.61	1.97	1.49	^q	^q	^q
NCI-H226	1.89	1.69	1.60	3.31	18.6	3.72	1.71	3.40	1.52	1.93	1.66	2.32	1.54	2.0	1.55
NCI-H23	3.04	2.15	3.04	2.02	23.4	2.60	2.48	4.12	2.90	1.97	2.25	4.21	2.47	3.22	1.87
NCIH322M	1.92	1.52	2.00	3.01	14.5	3.37	2.23	2.48	2.09	2.02	2.67	4.34	1.62	1.84	1.54
NCI-H460	1.72	1.41	1.89	2.12	4.9	2.96	1.80	1.81	1.81	1.04	0.60	2.03	1.64	2.07	1.68
NCI-H522	1.47	0.18	0.52	1.03	1.33	1.57	1.62	1.82	1.59	1.33	1.69	1.65	0.41	1.21	0.25
<i>Colon</i>															
COLO-205	1.73	1.74	1.75	1.87	1.26	1.69	1.74	3.84	2.08	1.75	1.55	1.88	1.76	1.85	1.70
HCC-2998	1.78	2.13	1.83	1.95	9.56	3.69	2.01	4.99	2.02	1.90	1.74	2.02	2.02	1.83	1.88
HCT-116	1.73	0.88	1.31	1.85	2.95	4.00	1.10	2.43	1.90	0.42	0.36	1.71	1.01	1.38	1.03
HCT-15	1.58	1.27	1.50	2.12	4.29	3.01	1.37	2.81	1.95	1.19	1.09	1.70	1.35	1.00	1.12
HT29	1.97	1.62	1.79	2.18	1.15	2.62	1.85	2.98	2.45	1.30	1.38	2.60	1.55	2.75	1.45
KM12	1.56	1.07	1.49	1.76	3.37	3.06	1.41	2.86	1.86	0.78	0.62	1.68	1.38	1.54	1.29
SW-620	1.62	1.37	1.59	2.47	8.63	3.42	2.05	2.05	1.62	1.50	1.50	2.50	1.35	1.69	1.35
<i>CNS</i>															
SF-268	1.99	1.82	1.94	2.97	13.7	3.15	1.69	2.53	2.45	1.68	2.09	1.89	1.94	1.81	1.63
SF-295	^q	^q	^q	^q	^q	^q	2.55	2.51	2.58	1.67	1.60	3.58	2.08	3.09	1.64
SF-539	1.62	1.27	1.29	2.07	4.31	3.76	1.30	1.91	1.33	0.30	0.52	1.73	1.27	1.47	1.27
SNB-19	1.51	1.42	1.66	4.30	9.83	3.64	2.34	3.20	2.34	1.80	1.67	4.36	1.88	2.29	1.55
SNB-75	1.49	1.23	1.54	2.01	8.70	2.90	^q	1.98	2.40	1.31	1.16	2.74	1.55	2.25	1.65
U251	^q	^q	^q	^q	^q	^q	1.42	1.58	1.21	1.24	1.20	1.74	1.11	1.24	1.09
<i>Melanoma</i>															
LOX IMVI	1.58	1.38	1.52	1.82	3.39	3.18	1.06	1.97	^q	1.46	1.29	1.92	^q	^q	^q
MALME-3M	1.86	1.99	1.86	4.42	29.2	2.96	2.05	7.32	1.85	2.32	2.59	6.72	1.62	2.18	1.74
M14	2.20	1.84	1.79	3.86	18.2	2.70	1.83	6.36	2.91	1.80	1.91	2.28	2.17	2.67	1.82
MDA-MB-435	2.20	1.34	1.49	2.39	5.65	2.88	1.66	3.03	2.28	1.78	1.72	2.53	1.84	2.24	1.73
SK-MEL-2	4.14	1.85	1.96	10.3	13.9	2.30	2.85	6.93	^q	2.69	2.46	8.44	^q	^q	^q
SK-MEL-28	2.12	1.78	1.82	2.48	18.5	5.31	1.86	5.76	1.92	1.91	1.82	2.14	1.65	1.87	1.89
SK-MEL-5	1.72	1.65	1.57	4.51	13.4	2.27	1.65	6.74	3.32	1.58	1.58	3.16	1.77	2.71	1.89
UACC-257	1.75	1.49	1.57	2.46	16.3	1.75	1.87	7.06	2.95	1.79	2.16	6.46	1.73	1.90	1.71
UACC-62	1.85	1.74	1.78	4.67	18.8	2.38	1.70	4.10	1.81	1.79	1.86	3.11	1.65	1.48	1.63
<i>Ovarian</i>															
IGROV1	2.21	1.80	3.14	5.00	24.0	3.62	3.20	2.79	1.99	2.72	3.13	4.56	1.57	2.27	1.89

OVCAR-3	1.74	1.68	1.75	3.38	6.99	2.39	1.57	2.02	1.71	1.59	1.96	1.92	1.19	1.25	1.41
OVCAR-4	2.20	2.69	1.45	3.80	10.8	2.20	1.40	2.11	0.88	1.62	1.92	2.68	0.59	1.08	1.11
OVCAR-5	1.88	1.59	1.64	3.37	20.5	4.48	1.78	3.36	2.63	1.76	1.76	2.62	1.65	2.06	1.56
OVCAR-8	2.43	1.32	1.58	2.85	6.30	2.88	2.39	2.15	2.35	2.55	2.63	2.95	2.16	2.44	1.57
NCI/ADR-RES	2.7	3.13	3.47	4.23	10.6	3.46	3.80	^g	2.99	2.69	3.43	6.21	3.44	2.86	2.25
SK-OV-3	3.99	2.79	3.20	5.76	4.19	3.53	2.99	3.97	4.44	5.47	3.13	4.86	5.56	4.72	2.89
<i>Renal</i>															
786-0	1.95	1.40	1.56	2.33	10.1	3.35	2.04	3.12	1.84	1.50	1.81	1.88	1.60	2.12	1.61
A498	1.74	1.48	1.61	2.76	5.89	2.11	1.64	1.55	1.75	1.46	1.27	2.37	1.42	2.03	1.33
ACHN	1.96	1.66	1.62	1.88	21.4	3.26	1.61	3.49	2.20	1.45	1.59	1.67	1.68	2.01	1.73
CAKI-1	2.34	2.20	2.58	5.51	16.9	2.98	^g	1.90	1.99	^g	^g	^g	1.55	1.32	1.50
RXF 393	1.27	1.35	1.26	1.48	2.70	2.05	1.35	2.42	1.31	1.53	1.92	2.15	1.39	1.67	1.54
SN12C	1.81	1.54	1.47	3.94	13.7	3.37	1.86	3.25	2.26	1.77	4.96	3.53	1.64	1.89	1.59
TK-10	2.22	1.33	1.46	2.33	8.34	2.29	4.84	2.88	2.90	3.27	1.50	1.09	2.11	2.81	1.89
UO-31	1.45	1.28	1.19	1.91	5.73	2.63	1.36	2.32	1.34	1.27	1.50	3.03	1.17	1.18	1.29
<i>Prostate</i>															
PC-3	1.51	1.36	1.47	2.81	5.95	1.66	2.21	2.58	1.51	1.99	1.98	3.71	1.45	2.42	1.29
DU-145	1.43	0.55	^g	2.72	^g	^g	1.65	1.86	2.92	1.83	1.64	3.74	1.40	1.32	1.45
<i>Breast</i>															
MCF7	1.15	0.82	0.64	1.67	1.80	3.20	1.50	3.27	1.06	1.06	0.93	2.28	0.41	0.78	0.33
MDA-MB-231/ATCC	1.88	1.48	1.52	3.50	8.65	1.64	2.06	2.44	2.08	2.02	1.88	4.42	2.00	2.14	1.66
HS 578T	3.60	2.57	2.68	3.71	16.6	3.58	4.33	2.69	3.14	2.91	3.76	6.57	3.38	4.04	2.61
BT-549	1.86	1.44	1.57	2.37	8.40	4.11	1.38	1.97	2.02	1.36	1.44	1.50	1.68	1.74	1.62
T-47D	2.31	1.63	1.13	2.51	1.66	2.45	1.42	3.23	1.51	1.01	1.36	4.25	1.60	1.47	1.31
MDA-MB-435	1.29	0.75	1.15	1.40	1.98	2.22	1.01	1.86	1.40	1.33	1.09	1.55	1.22	0.43	1.07

^aConcentration of the compound used to decrease cell growth to half that of untreated cells. ^b**13b** (NSC 765802/1), ^c**13c** (NSC 765806/1), ^d**13d** (NSC 765812/1), ^e**13e** (NSC 765805/1), ^f**13h** (NSC 765804/1), ^g**13i** (NSC 765808/1), ^h**13j** (NSC 774978/1), ⁱ**14c** (NSC 765828/1), ^j**14d** (NSC 768415/1), ^k**15a** (NSC 774980/1), ^l**15c** (NSC 774979/1), ^m**15d** (NSC 774981/1), ⁿ**16b** (NSC 768407/1), ^o**16d** (NSC 768408/1), ^p**18f** (NSC 768398/1), ^qNot tested.

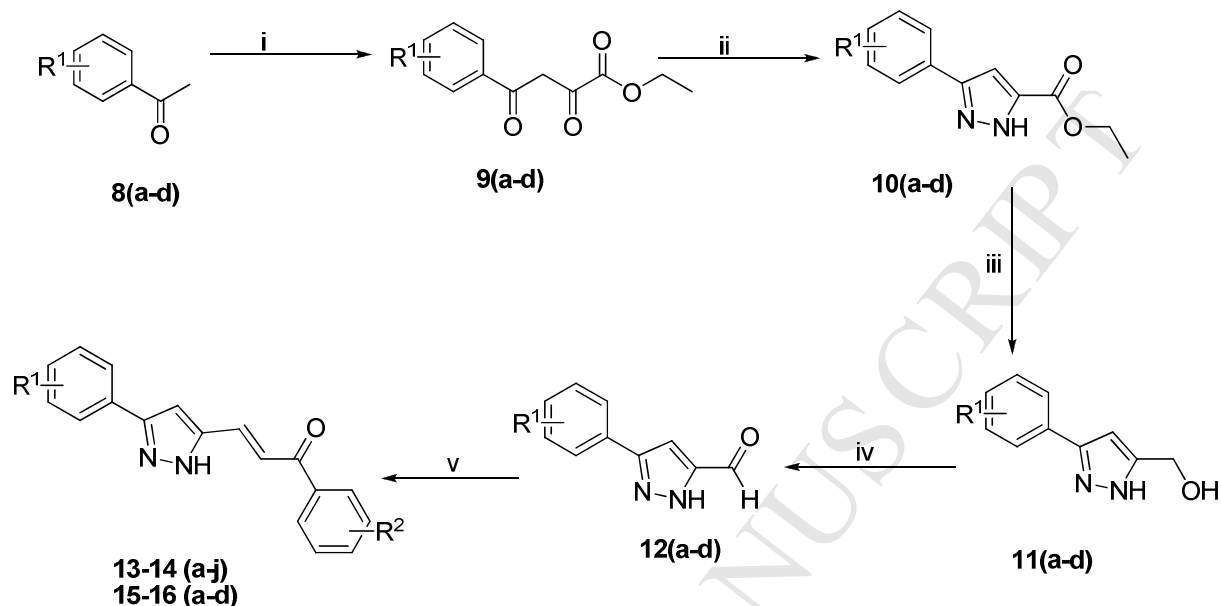
Table 2

		 13-14 (a-j) 15-16 (a-d)				 13-14 (a-j) 15-16 (a-d)			
Com pd	R ¹	R ²	IC ₅₀ (μM) ^a		Conju gates	R ¹	R ²	IC ₅₀ (μM) ^a	
			MCF-7 ^b	MDA-MB- 231 ^c				MCF-7 ^b	MDA- MB-231 ^c
13a		H	2.1 ± 0.12	2.3 ± 0.15	14e		3,4(-OCH ₂ O-)	2.1 ± 0.04	3.3 ± 0.16
13b		4-OCH ₃	0.81 ± 0.08	0.95 ± 0.1	14f	3,4(-	3-F, 4-OCH ₃	13.5 ± 0.93	15.9 ± 0.97
13c		3,4-(OCH ₃) ₂	0.51 ± 0.02	0.62 ± 0.01	14g	OCH ₂ O-)	4-Cl	15.0 ± 0.81	17.5 ± 0.83
13d		3,4,5-(OCH ₃) ₃	0.43 ± 0.03	0.70 ± 0.06	14h		3,4-(Cl) ₂	10.8 ± 0.64	14.8 ± 0.66
13e	3,4,5-	3,4(-OCH ₂ O-)	0.9 ± 0.05	1.72 ± 0.02	14i		3,4-(F) ₂	8.1 ± 0.09	12.1 ± 0.91
13f	(OCH ₃) ₃	3-F, 4-OCH ₃	3.0 ± 0.52	2.7 ± 0.38	14j		4-NH ₂	3.5 ± 0.07	5.1 ± 0.08
13g		4-Cl	11.6 ± 0.88	26.0 ± 0.98	15a		3,4,5-(OCH ₃) ₃	1.1 ± 0.04	2.0 ± 0.01
13h		3,4-(Cl) ₂	3.2 ± 0.45	2.1 ± 0.76	15b		3,4-(OCH ₃) ₂	0.8 ± 0.01	1.1 ± 0.06
13i		3,4-(F) ₂	2.5 ± 0.05	1.5 ± 0.23	15c	3,4-	3,4(-OCH ₂ O-)	1.5 ± 0.08	2.3 ± 0.08
13j		4-NH ₂	1.6 ± 0.03	2.0 ± 0.12	15d	(OCH ₃) ₂	4-NH ₂	1.9 ± 0.06	2.2 ± 0.05
14a		H	8.0 ± 0.61	12.1 ± 0.31	16a		3,4,5-(OCH ₃) ₃	2.0 ± 0.13	2.4 ± 0.11
14b	3,4(-	4-OCH ₃	3.5 ± 0.13	3.5 ± 0.12	16b	4-OCH ₃	3,4-(OCH ₃) ₂	0.5 ± 0.04	0.6 ± 0.03
14c	OCH ₂ O-)	3,4-(OCH ₃) ₂	2.5 ± 0.31	1.5 ± 0.21	16c		3,4(-OCH ₂ O-)	2.5 ± 0.08	3.3 ± 0.08
14d		3,4,5-(OCH ₃) ₃	0.85 ± 0.03	1.2 ± 0.06	16d		4-NH ₂	0.8 ± 0.06	1.7 ± 0.09
17a			20.1 ± 0.4	27.3 ± 0.86	18a			21.6 ± 0.93	20.2 ± 0.98
17b			10.1 ± 0.8	17.8 ± 0.92	18b			15.1 ± 0.89	11.8 ± 0.13
17c			8.5 ± 0.21	9.5 ± 0.71	18c			9.9 ± 0.41	12.6 ± 0.79
17d			4.8 ± 0.63	7.1 ± 0.08	18d			5.1 ± 0.13	8.3 ± 0.09

17e		2.1 ± 0.47	2.0 ± 0.04	18e		2.7 ± 0.09	4.1 ± 0.65
17f		2.0 ± 0.68	2.5 ± 0.21	18f		1.7 ± 0.18	1.6 ± 0.17
ADR		1.2 ± 0.08	1.8 ± 0.11	CA-4		0.12 ± 0.01	0.17 ± 0.02
^a Concentration required to inhibit 50% cell growth and the values represent mean \pm S.D. from three different experiments performed in triplicates. ^b MCF-7 and ^c MDA-MB-231: breast adenocarcinoma cell lines.							

Schemes

Scheme 1



	R ¹
13(a-j)	3,4,5-(OCH ₃) ₃

	R ²
13a	(H)
13b	4-OCH ₃
13c	3,4-(OCH ₃) ₂
13d	3,4,5-(OCH ₃) ₃
13e	3,4-(OCH ₂ O)
13f	2-F,4-OCH ₃
13g	4-Cl
13h	3,4-(Cl) ₂
13i	3,4-(F) ₂
13j	4-NH ₂

	R ¹
14(a-j)	3,4-(OCH ₂ O)

	R ²
14a	(H)
14b	4-OCH ₃
14c	3,4-(OCH ₃) ₂
14d	3,4,5-(OCH ₃) ₃
14e	3,4-(OCH ₂ O)
14f	2-F,4-OCH ₃
14g	4-Cl
14h	3,4-(Cl) ₂
14i	3,4-(F) ₂
14j	4-NH ₂

7(a-d) to 11(a-d)

a = R₁(3,4,5(OCH₃)₃) b = R₁(3,4-OCH₂O-)
 c = R₁(3,4,(OCH₃)₂) d = R₁(4-OCH₃)

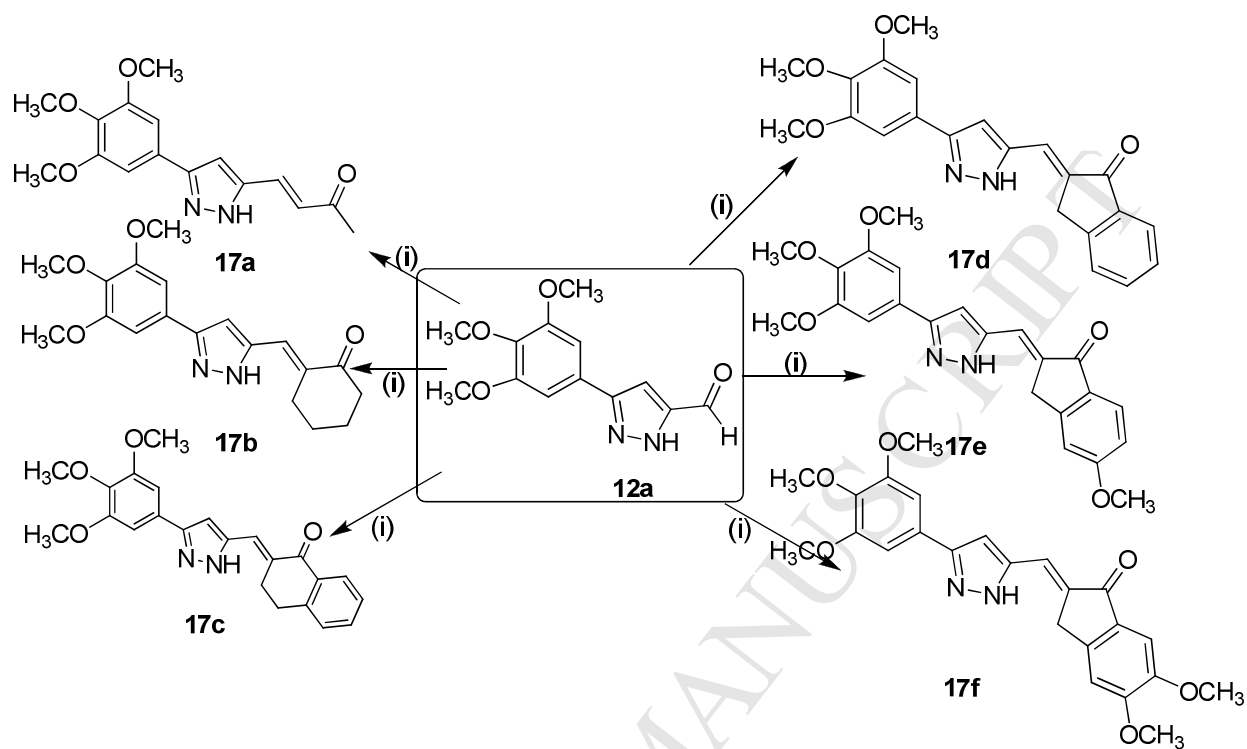
	R ¹
15(a-d)	3,4-(OCH ₃) ₂

	R ²
15a	3,4,5-(OCH ₃) ₃
15b	3,4-(OCH ₃) ₂
15c	3,4-(OCH ₂ O)
15d	4-NH ₂

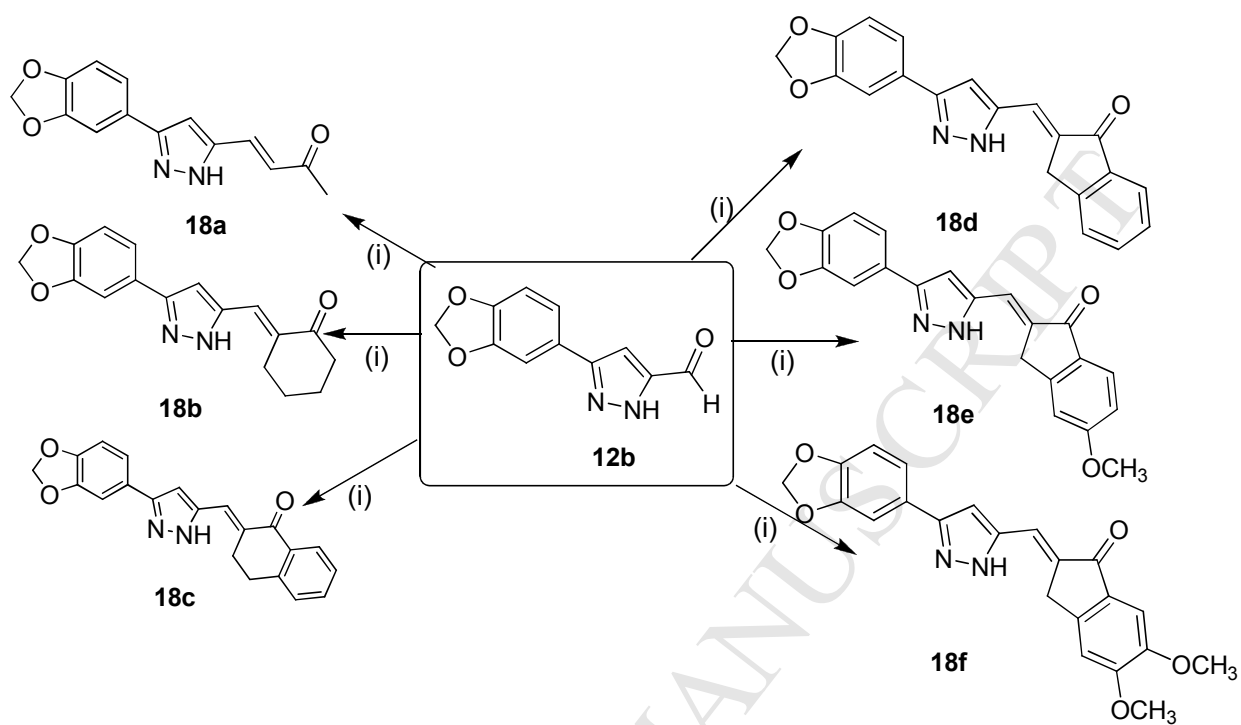
	R ¹
16(a-d)	4-OCH ₃

	R ²
16a	3,4,5-(OCH ₃) ₃
16b	3,4-(OCH ₃) ₂
16c	3,4-(OCH ₂ O)
16d	4-NH ₂

Scheme 2



Scheme 3

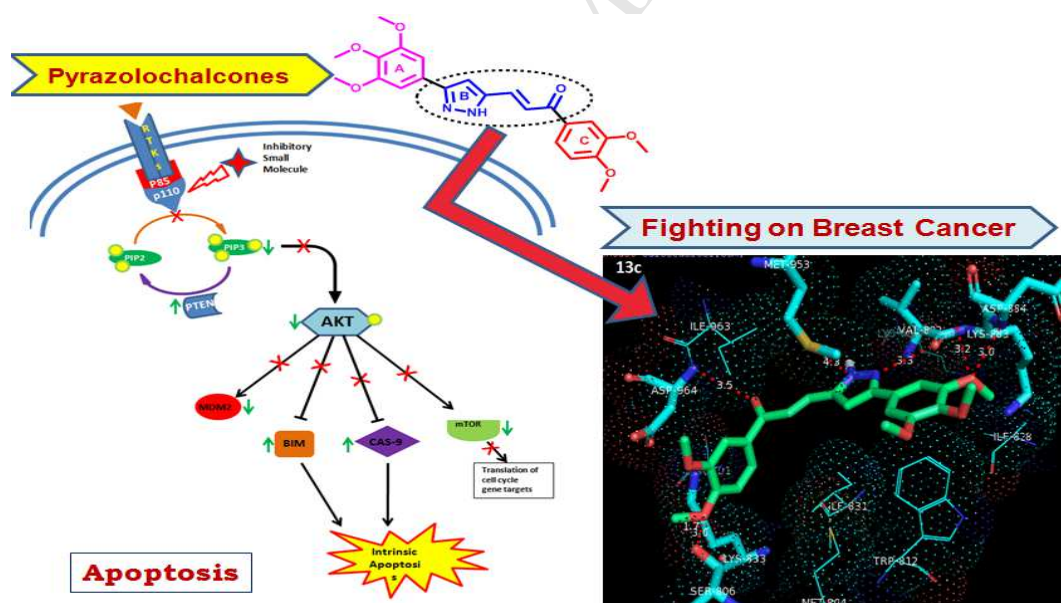


Graphical abstract

Design, Synthesis and Biological Evaluation of Novel Pyrazolochalcones as Potential Modulators of PI3K/Akt/mTOR Pathway and Inducers of Apoptosis in Breast Cancer Cells

Anver Basha Shaik,¹ Garikapati Koteswara Rao,² G. Bharath Kumar,¹ Nibeditha Patel,² Vangala Santhosh Reddy,¹ Irfan Khan,¹ Sunitha Rani Routhu,¹ C. Ganesh Kumar,¹ Immadi Veena,² Kunta Chandra Shekar,¹ Madan Barkume,³ Shailesh Jadhav,³ Aarti Juvekar,³ Jyoti Kode,^{*3} Manika Pal-Bhadra,^{*2} Ahmed Kamal^{*1}

A set of forty pyrazolochalcone conjugates and explored their cytotoxic activity against a panel of sixty cancer cell lines. Fifteen conjugates of the series showed excellent growth inhibition (13b-e, 13h-j, 14c-d, 15 a, 15 c-d, 16b, 16d and 18f; GI₅₀ for MCF-7: 0.4 – 20 μ M). Conjugates 13b, 13c, 13d, 16b and 14d were also evaluated for their cytotoxic activity in human breast cancer cell line (MCF-7).



Research Highlights

- Novel pyrazolochalcone synthesized and tested cytotoxic activity on sixty cancer cell lines. Most of them showed excellent growth inhibitory effect (GI_{50} for MCF-7: 0.4 – 20 μ M).
- The **13b**, **13c**, **13d**, **16b** and **14d** induced cell cycle arrest in G2-M phase of the cell cycle at 24 h and the conjugates **13c** and **14d** also accumulates in G0-G1 phase
- Induce mitochondrial membrane depolarization and apoptosis in MCF-7 cells.
- Inhibited PI3K/Akt/mTOR pathway-regulators and docked at the ATP binding site of PI3K.